report

# ERMS

Environmental Risk Management System

Program participants: - Agip - Conoco Phillips - Exxon Mobil - Hydro - Petrobras - Shell - Statoil - Total

STF80MK A06226 Open
Date: 31.08.2006

ERMS Report no. 21

# Restitution of an impacted sediment

Henrik Rye, Øistein Johansen, Ismail Durgut, Mark Reed, May Kristin Ditlevsen

SINTEF

**SINTEF Materials and Chemistry**

Address: NO-7465 Trondheim, NORWAY
Location: Brattørkaia 17B, 4. etg.
Telephone: +47 4000 3730
Fax: +47 930 70730

Enterprise No.: NO 948 007 029 MVA

# SINTEF REPORT

TITLE

## ERMS Report No. 21: Restitution of an impacted sediment

## Final report

AUTHOR(S)

Henrik Rye, Øistein Johansen, Ismail Durgut, Mark Reed and May Kristin Ditlevsen

CLIENT(S)

ERMS JIP

| REPORT NO. | CLASSIFICATION | CLIENTS REF. | |
|---|---|---|---|
| STF80MK A06226 | Open | ERMS Steering Committee | |
| CLASS. THIS PAGE | ISBN | PROJECT NO. | NO. OF PAGES/APPENDICES |
| Open | 82-14-03771-9 | 661367.70 | 41 |
| ELECTRONIC FILE CODE | | PROJECT MANAGER (NAME, SIGN.) | CHECKED BY (NAME, SIGN.) |
| ERMS report no 21_ Restitution_Final.doc | | Henrik Rye | Mark Reed |
| FILE CODE | DATE | APPROVED BY (NAME, POSITION, SIGN.) | |
| | 31 August 2006 | Tore Aunaas | |

ABSTRACT

As a part of the ERMS project (ERMS = *Environmental Risk Management System*), factors influencing on the restitution time of an impacted sediment are considered.

Three factors are considered in the present ERMS report:

- The biodegradation rates of chemicals in a sediment
- The re-suspension of particulate matter on the sea floor
- The recovery time for an impacted sediment

The main focus is directed toward modelling of the re-suspension of cuttings piles deposited on the sea floor. A numerical model for re-suspension has been developed, and results are compared to field data observations carried out at the North East Frigg and Frøy fields in the Frigg area of the North Sea.

| KEYWORDS | ENGLISH | NORWEGIAN |
|---|---|---|
| GROUP 1 | Dischargs to sea | Utslipp til sjø |
| GROUP 2 | Environmental impact | Miljøeffekter |
| SELECTED BY AUTHOR | Drill cuttings and mud | Borekaks og boreslam |
| | Risk analyses | Risikoanalyse |
| | Numerical modelling | Numerisk modellering |

# SUMMARY AND RECOMMENDATIONS

The present summary and recommendations covers the three chapters 2 (on oxygen consumption in the sediment), 3 (on re-suspension of sediment) and 4 (on re-colonization of a sediment layer).

***On oxygen consumption rates in the sediment***: The DREAM model was applied to simulate the oxygen balance for sediment as observed during laboratory trials. The laboratory trials as well as the model simulations show that the biodegradation rates of biodegradable matter in the sediment will be slowed down when there is a lack of oxygen in the sediment. This slowdown of biodegradation in the sediment may be considerable. It is therefore recommended that the biodegradation of the chemicals in the sediment is *not* assumed to follow the rates of biodegradation indicated by the HOCNF testing of the chemicals (where oxygen is not considered to be a limiting factor), but takes into account the availability of oxygen in the sediment. This reduction of biodegradation rates (availability of oxygen in the sediment layer) is presently built into the DREAM sediment model (by use of the "diagenetic equations").

***On re-suspension of added sediment:*** A module has been developed for DREAM that is able to re-suspend and re-distribute the particle matter deposited on the sea floor. The results from the module have been compared to measurements of remnants of cuttings piles at the Frigg field in the North Sea. Model results are sensitive to the input grain size distribution. Due to lack of data on grain size distributions for the matter that was deposited, it turned out to be difficult to verify the comparison between simulation results and the observed results. The DREAM re-suspension model as such is ready to be used, but at present it is recommended that activity-specific grain size distribution data for the discharge be used. The availability of field data will of course increase the reliability of model applications.

***On the re-colonization of impacted sediment layer:*** This study was limited to a literature review. It turns out that re-colonizations appear in successions, where different species dominate at various time intervals during the restitution of the sediment. Estimated times for re-colonization vary in the literature. Based on judgement, a re-colonization time of 5 years was recommended to be used in the DREAM model simulations until more information becomes available. A special case occurs when the discharges have changed the substrate of the sediment (change in median diameter of the sediment). Then a permanent change of community may occur due to the change of the substrate. In such a case, it is recommended that this new community is "accepted" after a time period of 5 years. It is therefore recommended built into the DREAM model that the grain size stress is reduced gradually over a time period of 5 years, assuming that no toxic stressors and no oxygen depletion are acting on the sediment. This recommendation is presently built into the DREAM model.

# TABLE OF CONTENTS

# 1 Introduction

## 1.1 General

The ERMS model calculates the deposition of the drill cuttings and the mud on the sea floor. This calculation forms the basis to evaluate the size of the area impacted by the discharge. However, the EIF method also requires an estimate of the duration of the impact on the sediment layer in order to estimate the time needed before the sediment layer is recovered back to normal. This restitution time expresses the time needed for the sediment to recover from the impact as defined by the four stressors: Burial, grain size change, toxicity and oxygen depletion. Assuming that this restitution is caused by natural processes, a number of natural processes will contribute to bring the sediment layer back to original conditions. Examples of such processes are:

- Biodegradation of organic chemicals in the sediment
- Re-suspension and re-distribution of matter on the sea floor
- Re-colonization of the biota after disturbance on the sea floor

The ERMS report on model documentation (SINTEF, 2006) focuses on calculation of the fates of the discharges during discharges, while the processes causing the recovery of the sediment have received less attention. During the ERMS "Rome workshop" held in September 2004, the need for verifying (some of) the input numbers used for calculating the restitution time was pointed out. Therefore, a supplementary report has been worked out, covering the processes mentioned above.

This report brings the results from a literature study and a simulation study on how existing data can be used to verify the sediment module with respect to three important features:

- The **biodegradation** rates for OBM and SBM in the sediment
- The rates for **re-suspension** and the re-distribution of cuttings piles due to currents and wave action
- The characteristic time for **re-colonization** of an impacted area

A fourth activity was also included in the present project for validation of the biodegradation routine in the sediment module. It turns out that the laboratory trials on biodegradation of chemicals in mud also include measurement of oxygen consumption for the sediment layer. This quantity is also an output from the sediment module. The oxygen consumption routine in the model can therefore be validated by comparing the oxygen consumption in the model with the oxygen consumption measured in the laboratory under similar conditions.

## 1.2 The biodegradation rates

The biodegradation rates are of importance for the restitution of the sediment layer. A large biodegradation rate will reduce the content of organic compounds in the sediment originating from different chemicals added to the mud. Therefore, these rates are important for assessing the proper recovery time for the biota in the sediment. It is important to bear in mind that SBMs was developed to pose low marine toxicity and to be biodegradeable whilst OBMs previously used contained various amounts of toxicorganic compounds. OBMs were prohibited from discharge on the NCS in 1992. The biodegradation also consumes oxygen and thus depletes the sediment layer for its content of oxygen. NIVA has done extensive testing of various types of drilling mud (OBM, SBM and WBM) at their laboratory facilities at Solbergstrand in the Oslofjord area. A

"mesocosmos" has been built for reproducing conditions at the sediment sites impacted by drilling discharges from the offshore industry. Results from these experiments have been collected and presented by NIVA in a separate report. This report has been edited as a separate ERMS report (NIVA, 2006). These results will therefore not be considered further in the present report.

### 1.3 Oxygen consumption rates

The NIVA measurements at Solbergstrand also include the consumption of oxygen due to the biodegradation of the chemicals in the drilling mud. The ERMS sediment model also includes the oxygen consumption in the sediment layer as one of the output parameters. Therefore, the ERMS sediment model may also be used to simulate the oxygen consumption rates observed in the sediment during (some of) the biodegradation trials carried out at Solbergstrand. Thus, the coupling between the (reduced) sediment oxygen content and the biodegradation rates observed in the laboratory can be compared with model simulations as well. This comparison can be used to verify (or validate) the ERMS sediment model. Results from these comparisons are accounted for in Chapter 2 of the present report.

### 1.4 Re-suspension of mud and cuttings particles from the drilling site

Another process that is important for the recovery time of a sediment layer is the effects from re-suspension of the deposits on the sea floor. At more shallow water depths (preferably shallower than about 150 m), re-suspension due to currents and wave action may re-distribute the cuttings and mud deposited on the sea floor. This re-suspension may contribute to the spreading of the discharge on the sea floor and thus impact on the restitution time of the sediment layer. Algorithms to describe this process have been implemented in the ERMS sediment model.

For a validation of the algorithms implemented, the results from the model simulation should be compared to field data. One area where surveillance of (re-suspended) cuttings piles has been carried out is at the Frigg field in the North Sea. Here WBM has mainly been used, but some of the locations in the Frigg area have also used SBM and OBM. This difference in types of mud used may also have some impact on the re-suspension process because the OBM and SBM types of mud may cause the particles in the mud to stick together and thus reduce the impacts from the waves and the currents.

The results from the comparison between the field data results and the model simulation results are presented in Chapter 3 of the present report.

### 1.5 Re-colonization

In areas where the biota in the sediment has been impacted due to a cuttings and mud discharge, a re-colonization should take place before the sediment is considered restored. Numbers and agreement upon what type of benthic fauna that can constitute a re-colonized sediment are then needed in the model for the time duration of such a process. Due to large natural variations, proliferation of opportunists specialised in degrading particularly SBMs and possible permanent changes in benthic fauna due to permanent change in the sediments particle size distribution, re-establishing of biomass or number of individuals could be an alternative therm compared to re-colonization.

A short literature survey has therefore been carried out. A discussion of these is given in Chapter 4 in the present report.

### 1.6 Organization of the report

This report covers different topics that are all related to restitution of a sediment layer. However, the chapters 2, 3 and 4 are not interrelated. Each of these chapters has been written independently of each other. The scopes of work for these topics have also been varying. As an example, the chapter on re-colonization (chapter 4) is just a literature review, and the chapter does not contain any results from analysis carried out as a part of the present project.

The chapters have therefore a “discussion” as the last section, while a “summary and recommendation” for all the chapters have been included in the front of the report (after the title page).

References are listed in Chapter 5.

# 2 Oxygen consumption rates in sediment

## 2.1 Introduction

The NIVA report on biodegradation rates for chemicals in sediment (NIVA, 2006) summarizes the biodegradation rates of various types of mud tested at the NIVA laboratory facility at Solbergstrand, Norway. NIVA has carried out a lot of experiments on the biodegradation of various types of drilling muds (both OBM, SBM and WBM are included) and calculated typical half-lives of the mud chemicals based on the biodegradation rates. These half-lives might then be used as a basis for calculating the reduction rates of chemicals in the sediment. These rates might, in turn, be used as a basis for estimating the time needed for a recovery of the sediment.

The biodegradation of the chemicals in the sediment is mainly caused by bacteria that break down the compounds in the chemicals into their single constitute like water, hydrogen and $CO_2$. These processes however require access to oxygen. This oxygen is taken from the oxygen in the pore water in the sediment. The biodegradation rates are therefore dependent of the availability of the free oxygen in the pore water. If there is a lack of free oxygen in the pore water (anoxic conditions), the biodegradation rates may be significantly reduced or go down to zero.

Therefore, the half-life estimates for chemicals in the sediment based on biodegradation rates will be dependent on the oxygen content in the sediment. NIVA, in their report, also points out that the biodegradation process may be slowed down due to lack of oxygen available in the sediment layer. A direct interpretation of the NIVA biodegradation rates measured at Solbergstrand may therefore lead to results that are not correct or misleading in the case that the availability of the oxygen in the sediment layer is not taken into account.

One process that will bring new oxygen into the sediment layer is the presence of a diffusive flux of oxygen from the sea water above (which will typically contain oxygen with concentrations of order 6 – 10 mg/L) and down into the sediment layer through the pore water. This flux of oxygen is measured during the NIVA experiments at Solbergstrand. This flux of oxygen is also calculated in the ERMS sediment model. Therefore, there is an opportunity to compare the oxygen fluxes measured with the oxygen fluxes calculated with the ERMS model for the same model setup. This comparison may be used to verify or validate the use of the ERMS model for calculation of biodegradation rates and half-lives of chemicals in the sediment.

## 2.2 Approach chosen

The ERMS model for the sediment has taken the time variability of the biodegradation processes of chemicals in the sediment into account. The biodegradation process is simulated directly by means of the diagenetic equations as explained in Chapter 5 in the model documentation report (SINTEF, 2006). The diagenetic equations contain one equation for the breakdown of the hydrocarbon molecules into $CO_2$ and other constitutes. Another diagenetic equation is included for the oxygen consumption within the sediment layer. The transport of new oxygen through the pore water from the sea water above is included in the diagenetic oxygen equation as well. The equations are constructed such that both the chemical biodegraded and the oxygen concentration in the sediment layer are calculated as a function of the sediment depth (z) and time (t) within the

deposited area. Therefore, the slowdown of the breakdown processes of the chemical(s) in the sediment due to lack of oxygen is simulated by the ERMS model.

The actual transport of the oxygen into the sediment layer can be calculated from the equation (see chapter 5 in the SINTEF 2006 report on model documentation):

$$\text{Influx of } O_2 \text{ to sediment layer} = \varphi \frac{D_0}{\theta^2} \frac{\partial O_2}{\partial z} \qquad (2.1)$$

where

$\partial$ = the partial derivative symbol
z = the vertical dimension
$O_2$ (z, t)= the oxygen pore water concentration, g/m$^3$ (or mg/L) pore water
$D_0$ = diffusion coefficient for oxygen in pore water, cm$^2$/hour
$\theta$ = tortuosity of the sediment (-)
$\varphi$ = porosity of the sediment (-)

The formula shows that the influx of oxygen is proportional to the vertical oxygen gradient $\partial O_2 / \partial z$. The oxygen gradient is estimated at the sediment interface between the sediment layer and the sea water above. The oxygen influx is given per time step and per unit area of the sediment surface (adjusted for the porosity). This flux should match (approximately) with the consumption of the oxygen (production of the $CO_2$) due to the biodegradation processes.

The comparison with the laboratory data is then obtained by mimic the laboratory setup with the model (deposition depth and content of chemicals within the added sediment) and then run the ERMS model in order to observe to what extent the measured properties (like inward oxygen flux) equal the same quantity in the model.

Since formula (2.1) predicts that the downward flux of oxygen is basically dependent on the oxygen concentration gradient at the sea surface, it is possible to make an estimate of this downward flux. Assume, for typical values, that

$\partial z$ = the vertical increment = 1 mm
$\partial O_2$ = the change of $O_2$ over the increment of 1 mm vertical distance
$D_0$ = diffusion coefficient for oxygen in pore water = 2 x 10$^{-5}$ cm$^2$/s
$\theta^2$ = tortuosity of the sediment squared = 2
$\varphi$ = porosity of the sediment = 0.6

where values chosen are typical values based on Berner (1980) and Boudreau (1997).

Figure 2.1 shows the dependency of the inward flux of oxygen on the oxygen concentration gradient at the sea – sediment interface:

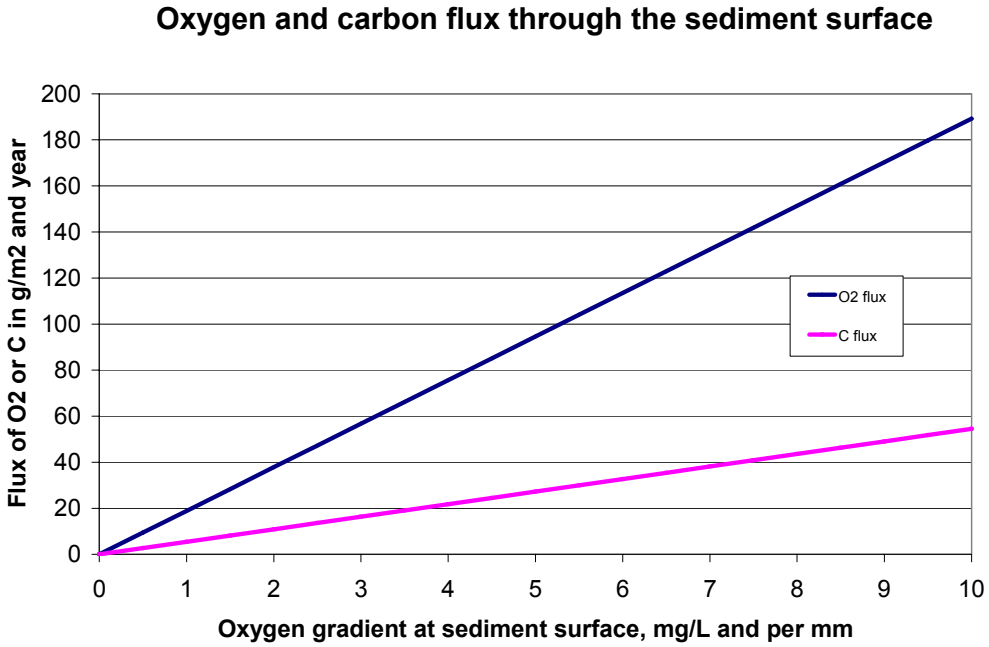


*Figure 2.1. The dependency of the oxygen flux (from the sea water into the sediment) on the vertical oxygen gradient across the sediment surface. The figure illustrates the results when the vertical increment is 1 mm. The flux of oxygen is derived from equation (2.1) and is directed downwards. The flux of carbon consists of $CO_2$ and is directed upwards.*

The figure shows that when the oxygen gradient is large (say, 8 mg/L over the upper mm for the sediment layer), the inward flux of oxygen is large (order 150 g $O_2/m^2$ sediment surface over one year). The flux is decreasing linearly with decreasing gradient of the oxygen concentration. This means that the laboratory measurements of the flux of the oxygen consumed by the sediment layer (the quantity at the left hand axis in Figure 2.1) can be approximated by an oxygen gradient at the sea surface.

The oxygen transported downwards across the sediment surface is consumed through biodegradation of organic carbon in the sediment. The carbon in the sediment is biodegraded to $CO_2$, which then diffuses upwards through the pore water. The conversion factor between oxygen and carbon due to biodegradation equals 12/32 (the molecular weights of C and $O_2$) times the factor 106/138 (Shimmield et. al., 2000). As an example, the carbon flux upwards due to biodegradation is equal to about 40 – 45 g $C/m^2$ sediment surface and year for the case that the gradient of oxygen across the sediment surface is about 8 mg/L over the upper mm of the sediment layer.

A gradient of the oxygen equal to about 8 mg/L change over the upper mm of the sediment layer means that the oxygen content in the sediment layer goes to zero more or less within the upper mm of the sediment layer. These consumption rates or vertical gradients of the oxygen in the pore water are occasionally observed, both in the field (Shimmield et al., 2000) and in the laboratory (NIVA, 1997 and SINTEF, 1999). The oxygen consumption measured by NIVA in various cases is a consumption rate of about 1 mol oxygen consumption per $m^2$ sediment surface over about 90 days. This is for sediments added with esters and olefins (NIVA, 1997). Similar numbers are reported by SINTEF (SINTEF, 1999), who measured an oxygen consumption of about 1.7 mol $O_2$ per $m^2$ sediment surface over a time period of 25 weeks. Both these numbers (which can be converted to about 130 and 110 g downward transport of oxygen per $m^2$ and per year or 0.36 and

0.30 g downward transport of oxygen per $m^2$ and per day) are reasonably close to the number reported by Shimmield et al., 2000 (151 g $O_2$ per $m^2$ and year or 0.41 g $O_2$ per $m^2$ and day).

This transport rate will represent a typical maximum consumption rate of oxygen in the sediment layer, causing the oxygen in the sediment to approach zero level within the upper mm of the sediment layer. For cases where the oxygen consuming matter is located deeper into the sediment layer, the downward flux of oxygen will be lower because the oxygen gradient (see equation 2.1) will be lower.

### 2.3 Results

NIVA has carried out their testing of different types of mud at their facility at Solbergstrand at the Oslofjord, Norway. Mud samples from supplier are mixed with sediment and then added on top of natural sediment stored in a 48 cm x 48 cm chamber (horizontal section). Then the biodegradation processes are monitored in the lab over a time period of 90 days.

The case that was reproduced in the ERMS model was a case with a deposition of 4 mm cuttings where a SBM type chemical (an ester chemical) was mixed into the sediment. Then the oxygen consumption rate was measured during the biodegradation process for two different temperatures (close to 7 $^oC$ and below 0 $^oC$).

Simulation of oxygen consumption was carried out by the sediment module which solves a set of diagenetic equations (SINTEF, 2006). The following basic parameters are applied in numerical model simulations carried out for the comparison:

Release profile: Cuttings are attached with a chemical.
Cuttings have one grain size (2mm) and the density of 2.65 g/cc.
Chemical has the density of 1.15 g/cc and the degradation rate coefficient of 0.0385 $days^{-1}$ (which corresponds to a half life of 18 days.
Release amount: 44 tons of cuttings released over a single sediment cell in the model (98m x 106m) in order to make 4 mm of deposition (with an assumed 0.6 porosity). Release has also 1980 kg of chemical (which will make an initial concentration of 190 $g/m^2$).
Porosity of both natural and added sediment: 0.6
Grain size of natural sediment: 1 mm

The history of oxygen flux calculated with the simulation model is shown in Figure 2.2. The numerical model updates the degradation rate by the presence (or absence) of oxygen in the sediment column. In the model, the bioturbation coefficient is corrected for risk factors caused by burial, oxygen depletion and toxic concentration in the sediment cell. In the present case, the depletion of the oxygen causes a reduced biologic activity (bioturbation coefficient) in the numerical model.

The experimental results for the oxygen influx (consumption) are between 300 $\mu \cdot mol/m^2/h$ (which is equivalent of 0.23 $g/m^2$ and day) and 1000 $\mu \cdot mol/m^2/h$ (0.77 $g/m^2$ and day). The average value is close to 500 $\mu \cdot mol/m^2/h$ (0.38 $g/m^2$ and day). The average value measured is therefore somewhat higher than the calculated value of order 0.25 – 0.30 $g/m^2$ and day.

The cumulative oxygen influx for the first 90 days in the numerical model simulation is shown in Figure 2.3. The amount of oxygen consumed in this time period is about 24 $g/m^2$. The laboratory

results show that this figure reaches, in average, up to 1000 m·mol/$m^2$ (32 g/$m^2$) in 90 days. However, the laboratory values vary between 800 m·mol/$m^2$ (25.6 g/$m^2$) and 1200 m·mol/$m^2$ (38.4 g/$m^2$).

Although this cumulative flux plot is given for the first 90 days, the model has been run for a longer period (1 year) to find out the half life of the added chemical. Figure 2.4 shows the calculated time history of oxygen flux for that time period.

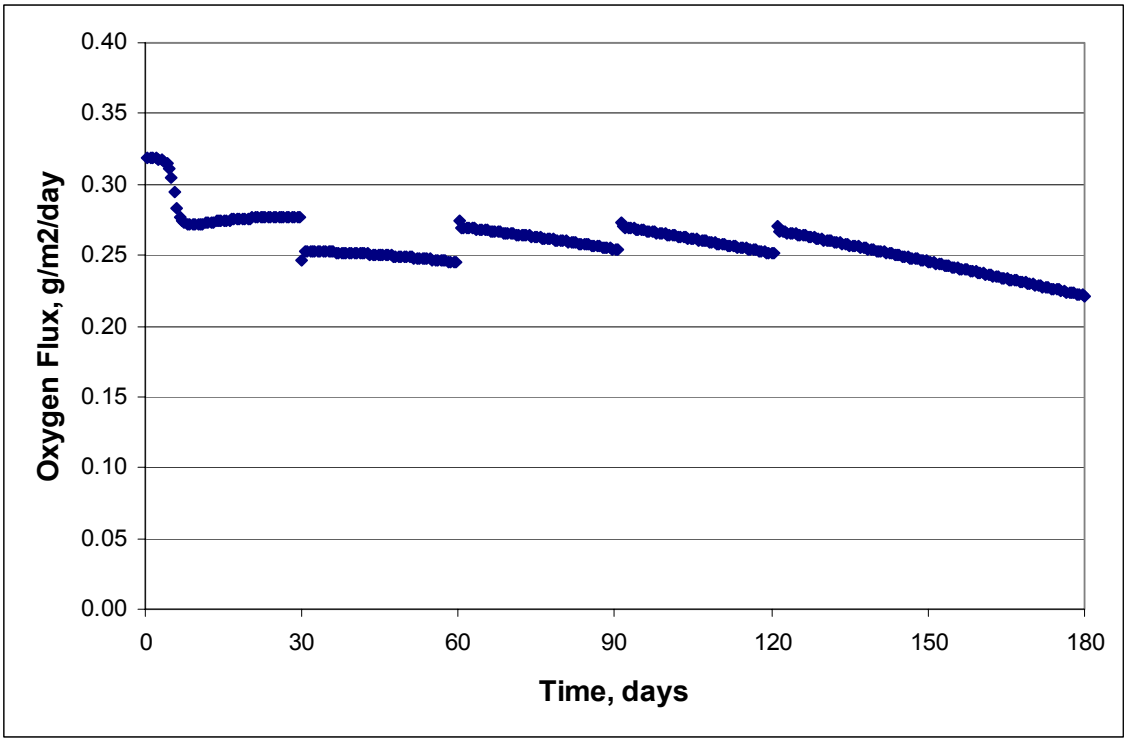


*Figure 2.2. – Oxygen flux history for the first 180 days modeled with the diagenetic equations.*

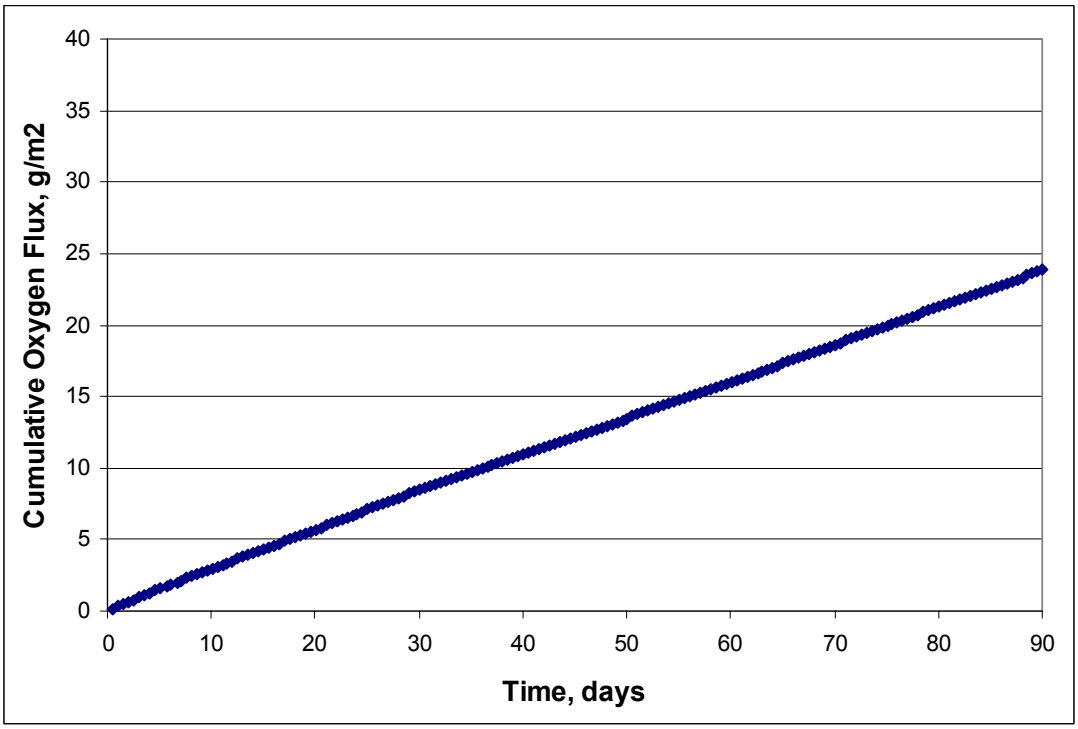


*Figure 2.3. – Calculated cumulative oxygen flux history for the first 90 days*

Figure 2.4 shows the time history of the oxygen consumption in the sediment layer modeled. The consumption rate tends to decrease after a time period of about 100 – 150 days. The explanation for this is that the chemical concentration in the sediment layer tends to be reduced close to the sediment surface due to the biodegradation. When the organic matter is biodegraded, the content of oxygen will tend to to rise again close to the sediment surface. Then the oxygen gradient at the sediment interface tends to be reduced, and the oxygen flux reduces, according to equation (2.1).

The time development of the concentration of chemical in the sediment as well as the oxygen concentration in the sediment are both shown in Figure 2.5. The model simulates the vertical concentration profiles of added chemical and oxygen. Figure 2.5 shows those profiles at zero day (just after adding the cuttings together with chemical), and at day-1, day-5, day-10, day-30, day-90 and day-365.

The model also calculates the half life of the chemicals remaining in the sediment layer. Figure 2.6 shows how the chemical is degraded during one year. From the plot, the half life can be estimated to be close to 250 days. The experimental values vary between 198 and 340 days (temperature dependent). Therefore, the model seems to reproduce the measured half-life of the chemical reasonably well.

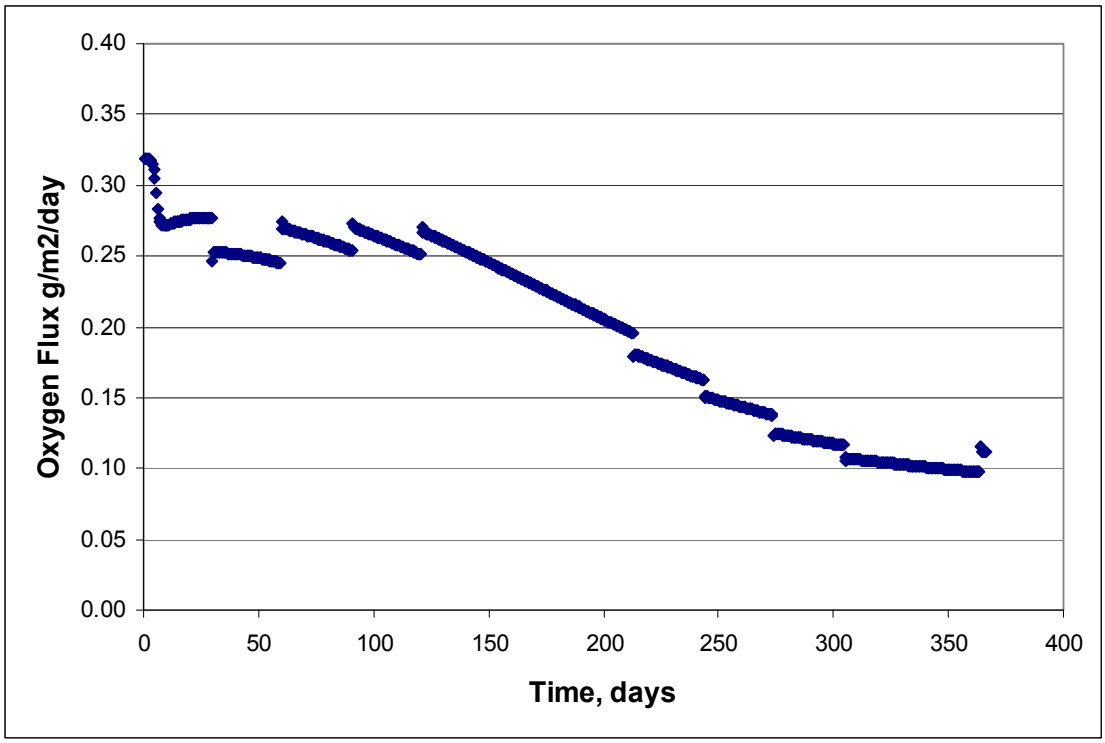


*Figure 2.4 – Oxygen flux history for a year, calculated with the model.*

One sensitivity study was added to the simulation runs. The numerical model uses porosity as an input parameter. For the cases shown above, the porosity was chosen to be 0.6. Another run was therefore included for the same case as shown above, except that the porosity was chosen to be 0.8 instead of 0.6. The resulting oxygen flux history is given in Figure 2.7. If the porosity is increased the oxygen flux will initially have higher values but will rapidly decline afterwards. Therefore, in order to reproduce the measured oxygen flux properly, information on the porosity is needed in addition.

## 2.4 Discussion

The model seems to reproduce the biodegradation of a chemical in sediment fairly well. The model is also able to reproduce the tendency for a chemical to have a variable half-life in the sediment, dependent on the oxygen consumption rate. Therefore, the model seems to be able to predict the restitution time of a sediment layer impacted by biodegradable matter. It should be stressed that the half-life of a chemical in a sediment cannot be represented by a single number, but will be dependent on the amounts deposited per $m^2$ surface area of the sediment layer and the oxygen consumption rate.

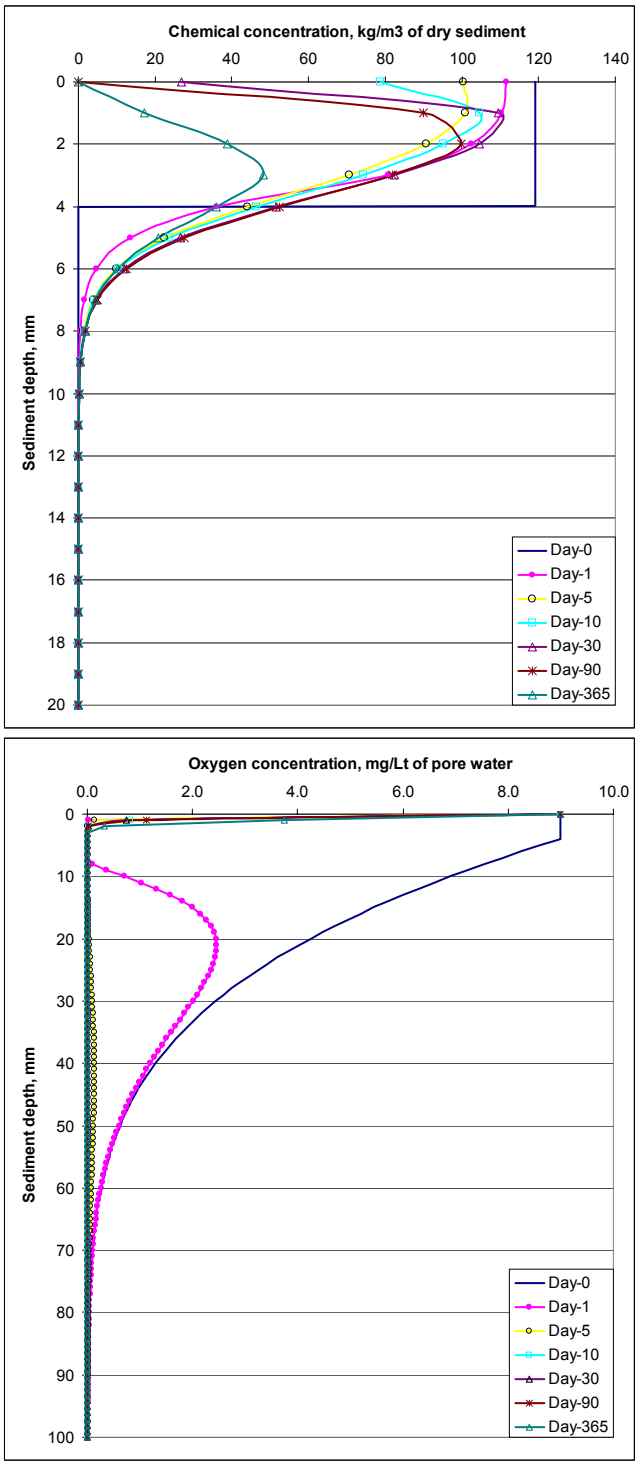


*Figure 2.5 – Concentration profiles for oxygen and chemical added at different times (day-0, -1, -5, -10, -30, -90, -365). The chemical is deposited at day 0.*

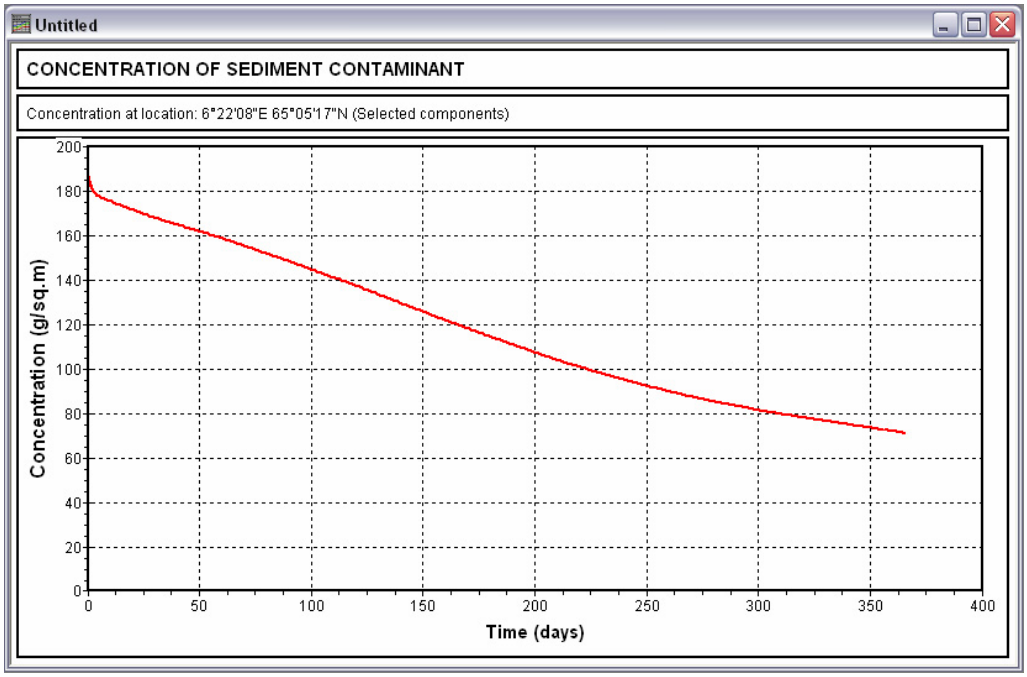


*Figure 2.6. – Concentration history of added chemical that remains in the sediment, computed with the model. The concentration in the sediment is reduced to about half its value after about 250 days.*

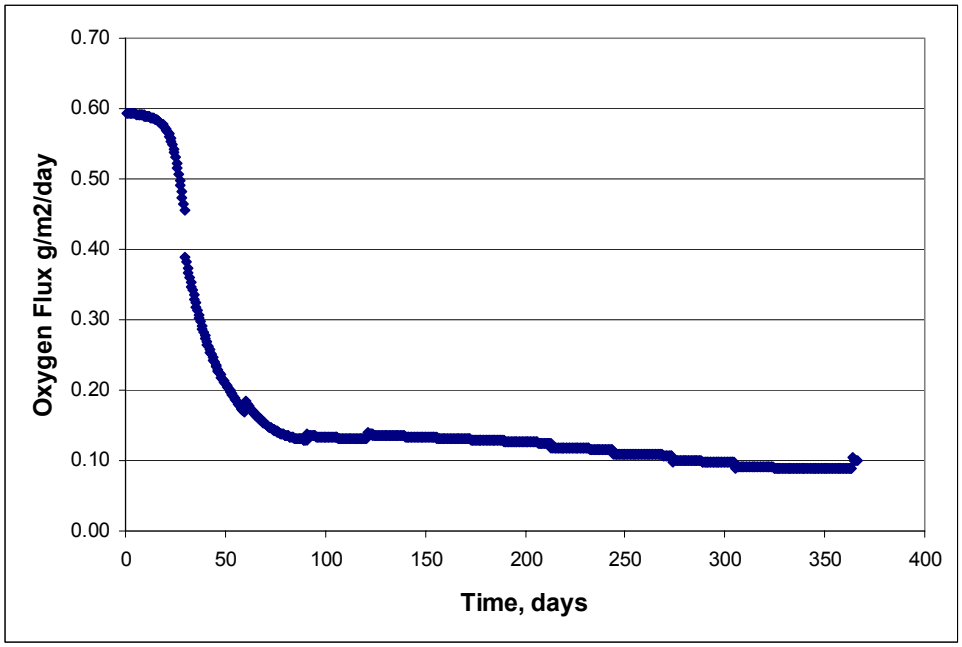


*Figure 2.7. – Oxygen flux history for the case of a porosity increase from 0.6 to 0.8. The oxygen flux is enhanced due to the increase in the porosity (and the decrease in the tortuosity) during the first 30 – 40 days.*

# 3 Re-suspension

## 3.1 Introduction

One of the processes that may impact on the restitution time of a sediment layer is the spreading of added matter on the sea floor under the action of winds and currents. The winds create waves that penetrate the water column and generate oscillating currents down on the sea floor. These oscillating water motions create stresses on the bottom surface that may cause deposited particles to be lifted off the ground. The (non-oscillating) currents will then move the added sediment in the main current direction until they settle again. The process may repeat itself several times, causing the added sediment to "move" away from the deposited area.

Such processes will have an impact on the restitution time of a sediment layer, because factors like burial (related to the thickness of the added sediment) and grain size (related to the median size of the grains on the sea floor) will be altered due to these processes. The impacted area may even be increased due to the spreading of the deposited matter. It is therefore important to have a realistic assessment of this spreading process in order to simulate the impacted area as well as the restitution time of the impacted sediment realistically.

Another requirement will be to have field data available that can be used to compare the model developed with field data. Such data sets exist for the North Sea area. As a part of the surveillance of cuttings piles in the Frigg and the Ekofisk areas, samples of the sediments have been collected from the areas where cuttings have been deposited previously. In this way, the thickness of cuttings piles has been determined after they have been exposed to waves and currents over a long period of time (years). By simulating the original deposition of the cuttings piles as well as the subsequent spreading of the cuttings on the sea floor (through re-suspension) throughout the years after, the resulting simulated thickness of the added sediment at the discharge site can be compared to the similar results based on the field data.

The data selected for comparison with model results has been collected at the Frigg field in the North Sea. Two fields were selected for comparison, one field where WBM has been used only (North-East Frigg) and one field that was drilled with SBM (Frøy WHP).

This part of the report starts with the theory applied for modeling the resuspension of the cuttings piles (Chapter 3.2). Then the implementation of the resuspension algorithms into the *DREAM/ParTrack/Sediment* model is given (Chapter 3.3). The next chapter then presents the data available from the two fields in the Frigg area for comparison as well as the input data used by the model (discharges, winds and ocean current data), Chapter 3.4. Simulation results and comparison with the field surveillance data are then shown for the North-East Frigg data case in Chapter 3.5 and for the Frøy WHP data case in chapter 3.6. A final discussion is included in Chapter 3.7.

## 3.2 Theory for the resuspension model

### Compute wave parameters from wind speed and fetch

A shallow water wave model from US Army Corps of Engineers has previously been used to compute significant wave height $H$ and peak period $T_p$ from surface wind and fetch $F$. A comparison with well established deep water wave models (JONSWAP) indicates that this model underestimates the peak wave period in deep waters, and this observation is confirmed

in the most recent update of the US Army Corps of Engineers Shore Protection Manual, (Section II – Meteorology and Wave Climate, updated July 2003) where it is stated that:

.., it is recommended that deepwater wave growth formulae be used for all depths, with the constraint that no wave period can grow past a limiting value (…) approximated by the relationship: $T_p = 9.78(D/g)^{1/2}$.

In this equation, $D$ is the water depth (m). The mentioned deepwater wave formulas are essentially equal to the JONSWAP formulas, with the exception that the model uses friction velocity $u_*$ instead of wind speed at 10 meter height, $U_{10}$. However, we have decided to use the original JONSWAP deep water wave formulas, expressed as:

$$\frac{gH}{U_{10}^2} = 0.0016\left(\frac{gF}{U_{10}^2}\right)^{1/2}$$ , limited to 0.243 for fully developed sea, and

$$\frac{gT_p}{U_{10}} = 0.286\left(\frac{gF}{U_{10}^2}\right)^{1/3}$$ , limited to 8.134 for fully developed sea, and eventually limited by the depth relationship for $T_p$ given above.

Figure 3.1 shows wave predictions for a range of wind speed and fetch based on these equations. For comparison, observed combinations of wave height and wave period from wave measurements at the Ekofisk area are shown in Table 3.1. By comparison, we find that the observed range in wave heights at a given range in wave periods are consistently larger than expected from the model predictions, and that wave heights is frequently observed below the fully developed sea condition. This may be explained by transients in the wave field, i.e. changes in wave conditions may lag after changes in wind conditions (falling and increasing sea state).

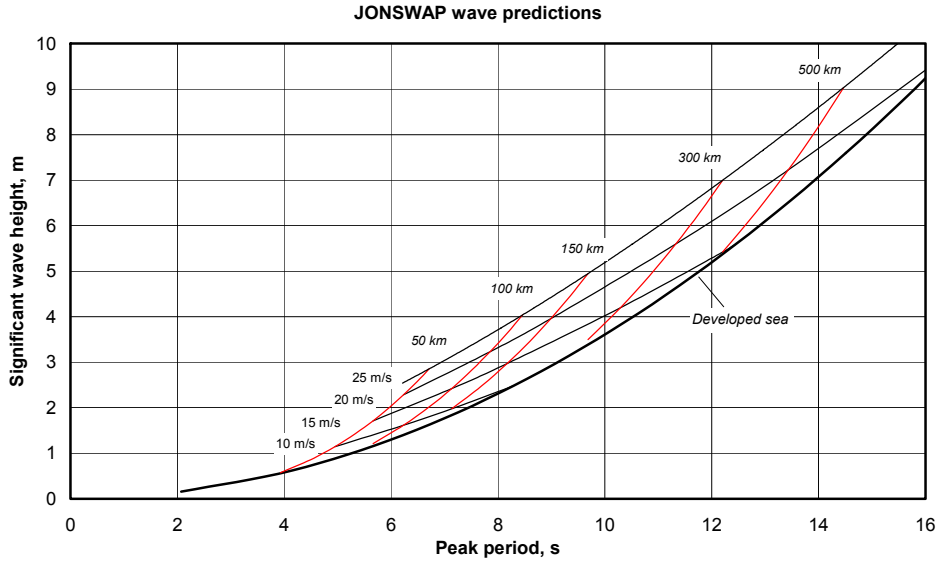


*Figure 3.1. Predictions of wave parameters from wind speed and fetch by the JONSWAP model. Black lines marked with wind speed shows values for constant wind and increasing fetch, while red lines shows values for constant fetch and increasing wind. The limiting case representing fully developed sea is shown by a bold black line.*

*Table 3.1. Joint frequency of occurrence of significant wave height and peak period from wave measurements in the Ekofisk area. Data from March 1990 to September 1993. Intervals of 1 seconds in wave period and 0.5 m in wave height. Values in*

*each cell represent number of measurements in each combined range. The yellow shaded area indicates the range in wave parameters shown in Figure 1.*

| | | Period, sec | | | | | | | | | | | | | | | | | |
|---|---|---|---|---|---|---|---|---|---|---|---|---|---|---|---|---|---|---|---|
| $H_s$, m | | < 4 | 4 5 | 5 6 | 6 7 | 7 8 | 8 9 | 9 10 | 10 11 | 11 12 | 12 13 | 13 14 | 14 15 | 15 16 | 16 17 | 17 18 | 18 19 | 19 20 | 20 21 |
| 0.0 | 0.5 | 83 | 162 | 62 | 45 | 58 | 53 | 34 | 34 | 17 | 5 | 8 | 10 | 1 | | 1 | 1 | | |
| 0.5 | 1.0 | 62 | 556 | 666 | 288 | 130 | 122 | 80 | 62 | 45 | 33 | 16 | 24 | 10 | 8 | 11 | | 1 | |
| 1.0 | 1.5 | | 86 | 500 | 501 | 248 | 105 | 43 | 37 | 44 | 23 | 5 | 11 | 4 | 9 | 12 | 1 | 1 | |
| 1.5 | 2.0 | | 4 | 108 | 369 | 351 | 159 | 39 | 36 | 50 | 36 | 12 | 9 | 6 | 3 | 4 | 2 | | |
| 2.0 | 2.5 | | | 17 | 148 | 283 | 187 | 43 | 12 | 19 | 19 | 13 | 2 | 1 | | | | | |
| 2.5 | 3.0 | | | 2 | 29 | 181 | 156 | 55 | 19 | 20 | 7 | 4 | 4 | 2 | 1 | | | | |
| 3.0 | 3.5 | | 1 | | 2 | 76 | 139 | 49 | 14 | 11 | 7 | 3 | 3 | 2 | | | | | |
| 3.5 | 4.0 | | | 1 | | 21 | 97 | 59 | 8 | 7 | 6 | 4 | | 1 | | | | | |
| 4.0 | 4.5 | | | | | 3 | 55 | 42 | 20 | 8 | 2 | 1 | 2 | | | | | | |
| 4.5 | 5.0 | | | 3 | | | 19 | 33 | 30 | 10 | 5 | 2 | 2 | 2 | | | | | |
| 5.0 | 5.5 | | | | | | 4 | 14 | 19 | 9 | 5 | 3 | 2 | | | | | | |
| 5.5 | 6.0 | | | | | | | 9 | 21 | 4 | 2 | 2 | 1 | | | 1 | | | |
| 6.0 | 6.5 | | | | | | | 2 | 11 | 7 | 2 | | | 3 | | | | | |
| 6.5 | 7.0 | | | | | | | 1 | 5 | 1 | 5 | 4 | 2 | 1 | 1 | | | | |
| 7.0 | 7.5 | | | | | | | | 3 | 5 | 5 | | 1 | | | | | | |
| 7.5 | 8.0 | | | | | | | | 1 | 3 | | | 1 | | 1 | | | | |
| 8.0 | 8.5 | | | | | | | | | 4 | 3 | | 1 | | | | | | |
| 8.5 | 9.0 | | | | | | | | | | 1 | | | | | 2 | | | |
| 9.0 | 9.5 | | | | | | | | | | | | | | | | | | |
| 9.5 | 10 | | | | | | | | | | 1 | | | | | | | | |

**Orbital velocity at sea bed**

The orbital velocity at a distance $z$ above the bottom with depth $D$ is computed from wave height $H$ and wave period $T$ by linear wave theory:

$$U_w = \frac{1}{2} H \omega \frac{\cosh(kz)}{\sinh(kD)} \approx H \omega \exp(-kD) \text{ at sea bed for large depths}$$

$$\text{where } \omega = \frac{2\pi}{T}, \quad k = \frac{\omega^2}{g \tanh(kD)} \approx \frac{\omega^2}{g} \text{ for large depths}$$

The orbital velocities are thus sensitive to the combination of wave height and period, and the probability for exceeding a certain limiting orbital velocity will thus be depending on the joint frequency distribution of the two parameters. To illustrate this dependency, we have made a comparison between bottom orbital velocities computed from (a) wave statistics based on wave measurements at the Ekofisk area, and (b) wave conditions predicted from hindcast wind data in the same area (Figure 3.2.). The results are may be considered to be in acceptable agreement, taking into account the limitations pointed out earlier in the wave prediction model.

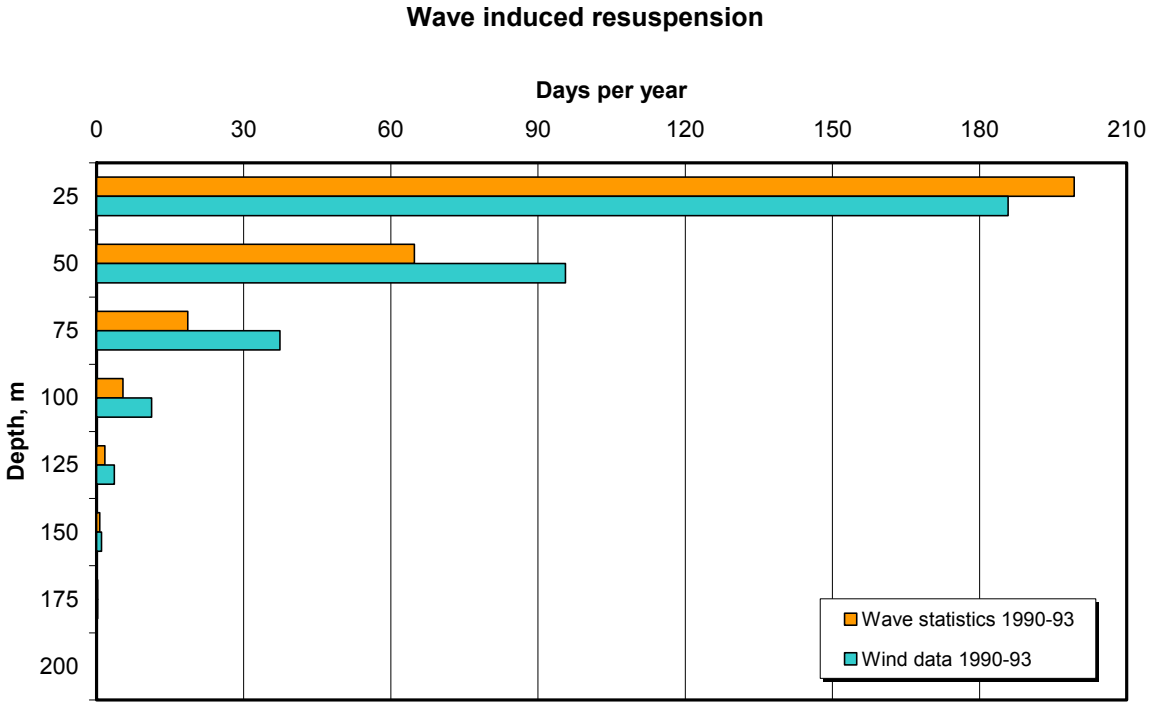


*Figure 3.2. Probability for exceeding sea bed orbital velocities of 20 cm/s computed from wave statistics (1990 – 1993) and hindcast wind data (1990 – 1993).*

**Bottom stress from currents and waves**

Bottom stress induced by currents is computed from a quadratic friction law:

$$\tau_c = \rho C_d U_z^2$$

where $\rho$ (kg/m$^3$) is the density of water, $C_d$ is the bottom drag coefficient, and $U_z$ (m/s) is the current referred to a distant $z$ above the sea bed. The value of the drag coefficient depends on the reference height $z$ of the current. According to Holloway and Barnes (1998), the drag coefficient is the maximum of 0.0025 and:

$$C_d = \left\{ \frac{\kappa}{\ln(z/z_0)} \right\}^2$$

where $\kappa = 0.4$ is the von Karman constant, $z$ is the distance above the sea bed, and $z_0$ (m) is the roughness height. Holloway and Barnes (1998) proposed a simple empirical relationship for the latter, $z_0 = 0.01 + 1/D$, where $D$ (m) is the local water depth, to account of increased roughness for shallow water.

The bottom stress induced by waves is related to the orbital velocity $U_w$ at the sea bed:

$$\tau_w = \frac{1}{2} \rho f_w U_w^2$$

where the wave friction coefficient $f_w$ is related to the orbital displacement length $A = U_w / \omega$ and the sediment roughness height $r = 2.5 d_{50}$, where $d_{50}$ (m) is the median grain size in the top sediment layer (the Swart's formula):

$$f_w = \exp\left\{ 5.213 \left( \frac{r}{A} \right)^{0.194} - 5.977 \right\}$$

It should be noted that Kuhrts et al. (2004) suggest an upper limit of 0.3 to this friction coefficient to avoid abnormally high values at conditions with very small orbital displacements.

**Critical Shields parameter**

The criteria for re-suspension is expressed in terms of a critical Shield parameter $\theta_c$, i.e. re-suspension will be initiated when $\theta > \theta_c$, and $\theta$ is a non-dimensional stress parameter:

$$\theta = \frac{\tau}{\rho(s-1)g\,d}$$

where $\rho$ is the density of water, $s = \rho_s / \rho$, g is the acceleration of gravity, $\rho_s$ is the density of the sediment particles, and $d$ the (median) sediment grain size. For combined wave and current bottom stress, the two shear stresses are simply added together, i.e. $\tau = \tau_w + \tau_c$.

The critical Shield parameter is found to be in the order of 0.04 to 0.05 for sandy sediments, but will in general depend on a friction velocity based Reynolds number, $\mathrm{Re}^* = u^* d / \nu$, where the friction velocity is defined as $u^* = \sqrt{\tau/\rho}$ (see Figure 3 next page). The empirical relationship shown at Fig. 3.3 can be fitted by a 4th order polynomial function $y = a_0 + a_1 x + a_2 x^2 + a_3 x^3 + a_4 x^4$, where $y = \theta_c$ and $x$ = ln (Re*), with the following fitted values of the coefficients:

$$a_0 = 0.109,\ a_1 = -0.0811,\ a_2 = 0.0276, a_3 = -0.0035, a_4 = 0.000152$$

It should be noted that the empirical values are based on experiments with non-cohesive materials, and that the correlation should not be used for cohesive material such as clay or oil based mud.

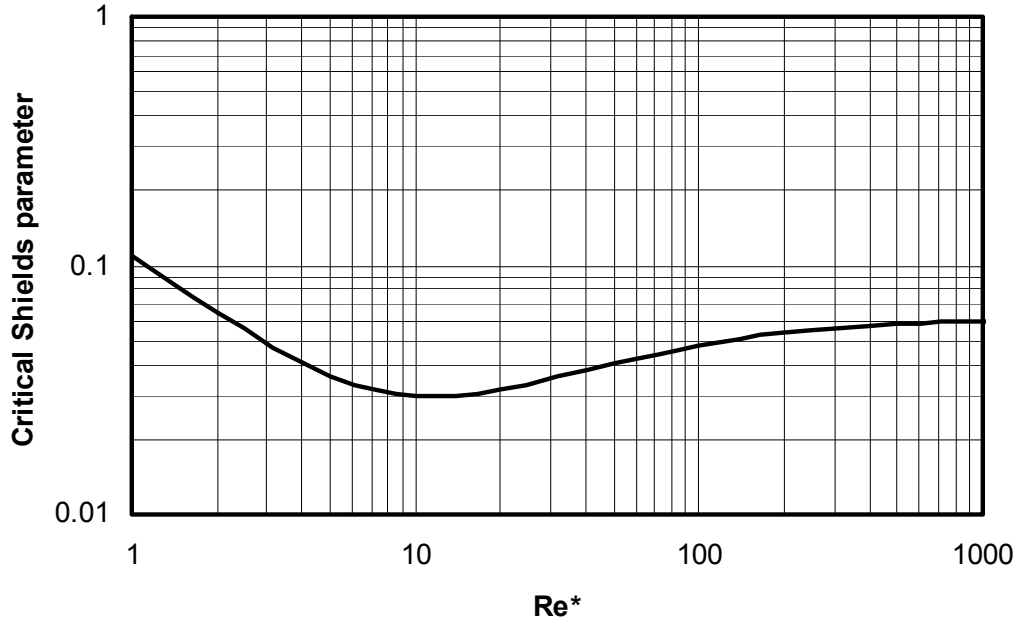


*Figure 3.3. Critical shield parameter shown as a function of the friction velocity based Reynolds number (Adapted from Fig. 7.6 in Fredsøe and Deigaard, 1992)*

**Re-suspension rate and vertical distribution**

Zyserman and Fredsøe (1994) developed the following empirical relation for the volumetric sea bed concentration ($m^3/m^3$):

$$C_0 = \frac{0.331(\theta - \theta_c)^{1.75}}{1 + 0.720(\theta - \theta_c)^{1.75}},$$

where $\theta = \frac{\tau}{\rho g' d_{50}}$, $g' = g(\rho_s - \rho)/\rho$, and $\theta_c$ is the critical Shield parameter

The pick up rate for each fraction in the sediment is, according to Black and Vincent, 2001:

$$P_i = F_i \, w_i \, C_0,$$

where $F_i$ is the mass fraction of grain size class $i$ and $w_i$ is the corresponding sinking velocity. The total pick-function is then the sum of all grain size classes:

$$P_i = \sum_{i=1}^{n} F_i \, w_i \, C_0 \,,$$

According to the same authors, the initial mixing height $L$ may be estimated as:

$$L = K_z / w$$

where $K_z$ ($m^2/s$) is the vertical diffusion coefficient at/near the sea bed, and $w$ (m/s) is the sinking velocity. We should use one mixing length for each size class, and distribute the emitted particles either exponentially or homogenously within this height.

Further mixing of the suspended sediments will be due to vertical turbulence. We have chosen to use Ichiye's formula (Ichiye 1967) for this purpose, i.e.:

$$K_z = 0.028 \frac{H_s^2}{T_p} \exp(-2\,k\,z)$$

where $z$ is vertical position of the sediment particle (depth below sea surface), $H_s$ is the significant wave height, and $T_p$ is the peak wave period.

**Secondary transport**

The advection routines already implemented in the present *DREAM/ParTrack/Sediment* model take care of this. Eventually, particles will settle to the sea bed, and must then be added to the sediment mass in the respective sea bed grid cell.

## 3.3 Implementation of the SINTEF resuspension model

The re-suspension model is developed in FORTRAN language as a part of FATES routine in the model system. It principally simulates re-suspension of sediment particles from sea bed induced by currents and wind. It follows the method described in the previous Chapter 3.2.

The model will be initiated and run if the check box called as "Resuspension of sediment" in the Sediment Model tab of Model Parameters' pages is checked.

The first step of the model is to read some (optional) input parameters. FATES will look for a file called RESUSP.DAT in the installation directory of MEMW. If the file exists and recognized (i.e. if it has a recognized file header) the input are read from the file. Otherwise (i.e. file not found), FATES runs with default parameters. The default values of parameters and their arrangement (the parameters follow free-format style of FORTRAN language) are given in the following figure:

```
!SINTEF 38 1 MEMW v3.0 Sep  1 2005
   3.0  ! maximum removal thickness (cm) - not used
 100.0  ! minimum mass to remove from a cell (mg/m2)
   1.0  ! minimum time step (min) - not used
   5.0  ! velocity multiplier for transport of resuspended sediment at bottom of sea
     3  ! number of part's resuspended from a cell for each part.mat.
```

*Figure 3.4. – Input file RESUSP.DAT*

The first and third parameters are not used (they were reserved for previous versions). The second parameter specifies the minimum removal from a cell. Resuspension will not take place if the mass to be removed is less than the given value. Since the model lacks an appropriate method to transport (to advect) resuspended sediment accordingly, it just advects with a given fraction of current velocity. The last parameter specifies how many particles will represent the resuspended sediment.

The algorithm creates number of particles for each type of particulate material from each sediment cell where the total bottom stress is above the critical value. The oil and chemical components are always attached to those particulate materials. If there is only chemical or oil deposited in a given cell the re-suspended stuff will behave as if attached to natural sediment (i.e. having grain size and density of natural sediment) but with the index of the 1$^{st}$ particulate material. Therefore if the release profile has no particulate material then there will be no re-suspension. The reason of this limit is not to be in a situation to follow re-suspended particles forever. In other words, the method makes use of resettling nature of re-suspended particles.

Re-suspended particles from a sediment cell are temporarily stored at the end of spillet (droplet) arrays. They go through only advection process. After one time step they are collected either in a list for particles resettled back or in another list for particles remained still in the water column. The algorithm utilizes linked list implementation to follow those particles. It creates two linked-lists. Particles in the list of resettled-ones go through the benthic process. Particles stored in the other list will be advected once in each time step until they resettle back to sediment.

The model has its own time-step which is set to the initial value of FATES' time-step. The resuspension algorithm is called once for every FATES' time-step. However, the algorithm may take additional steps if FATES' time step is longer (this may happen when the sediment model changes FATES' time step).

### 3.4 Input data for the simulation of the resuspension.

A surveillance of cuttings piles in the Frigg area was carried out by Rogaland Research in 1999 (Rogaland Research 2003, OLF 2001). A corer was used to penetrate the sediments close to the drilling site for collection of sediment samples down to maximum 30 - 50 cm depths. Reminiscences of the cuttings deposits were found, sometimes with a cap of local sand on the top. Figures 3.5 and 3.6 show a graphical representation of the results from the surveillance's at the North-East Frigg and the Frøy Wellhead Platform (WHP) locations, respectively.

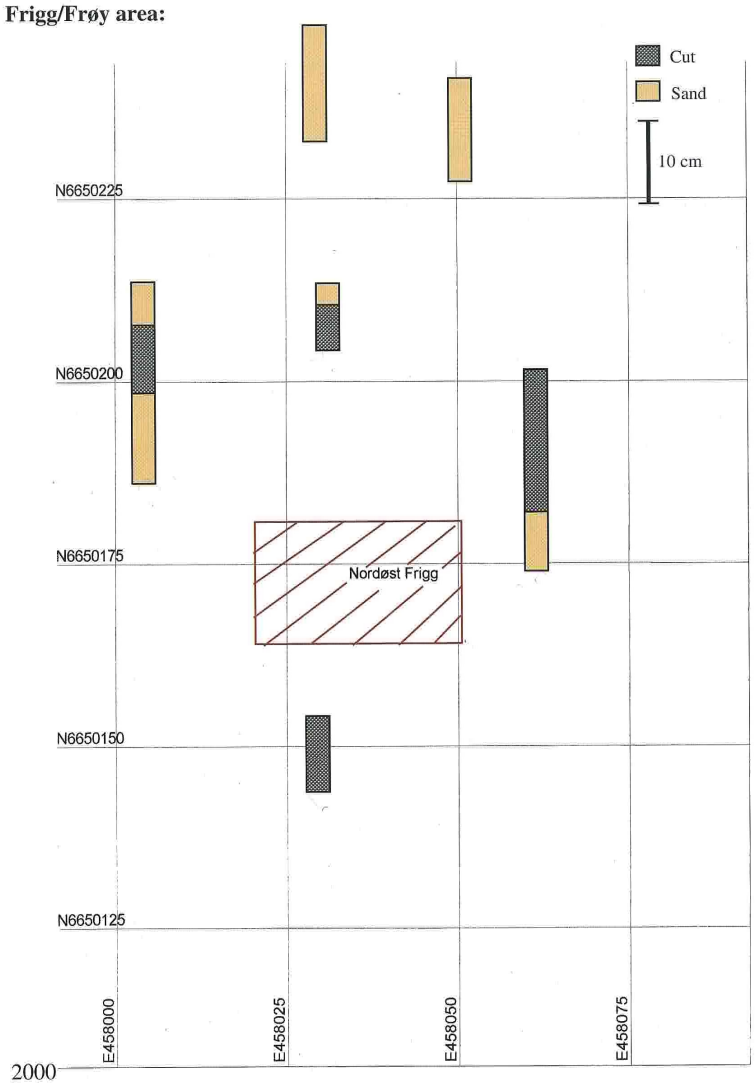


**Figure 1a**: Cores from North East Frigg with cuttings and sand layer shown. The installation shown on the map is removed. The grid on the map is in UTM co-ordinates.

*Figure 3.5. Results from measurements of cuttings that remain on the drill site at the North-East Frigg field in the North Sea. Reproduced from OLF (2001).*

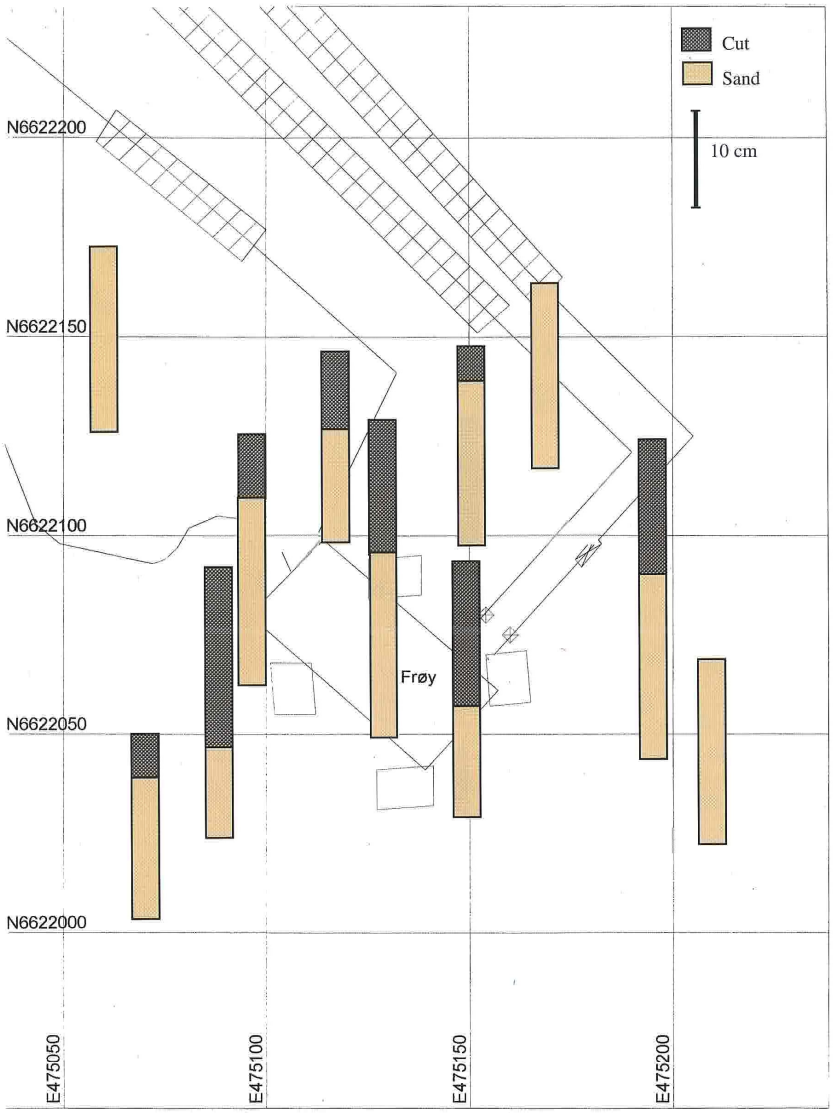


**Figure 1e**: Cores from Frøy WHP with cuttings and sand layer shown. Some of the cores are from the 1999 study. The drawing on the map shows the installation. The grid on the map is in UTM co-ordinates.

*Figure 3.6. Results from measurements of cuttings that remain on the drill site at the Frøy WHP field in the North Sea. Reproduced from OLF (2001).*

These cuttings piles were generated originally in the early 1980's (North-East Frigg case) and through the years 1993 - 95 (Frøy WHP case). Since then they have been dormant through the years, until they were surveyed in 1999. The two fields were satellites to the Frigg field and no other discharges than from drilling operations has taken place at the two sites.

The location of the cuttings piles are shown in Figure 3.7. They are located in the North Sea outside the western coast of Norway. Water depth in the North-East Frigg area is about 100 m and in the Frøy WHP area is about 120 m. These depths are sufficiently small for the fields to be exposed to impacts from both winds and waves, in particular through the winter season.

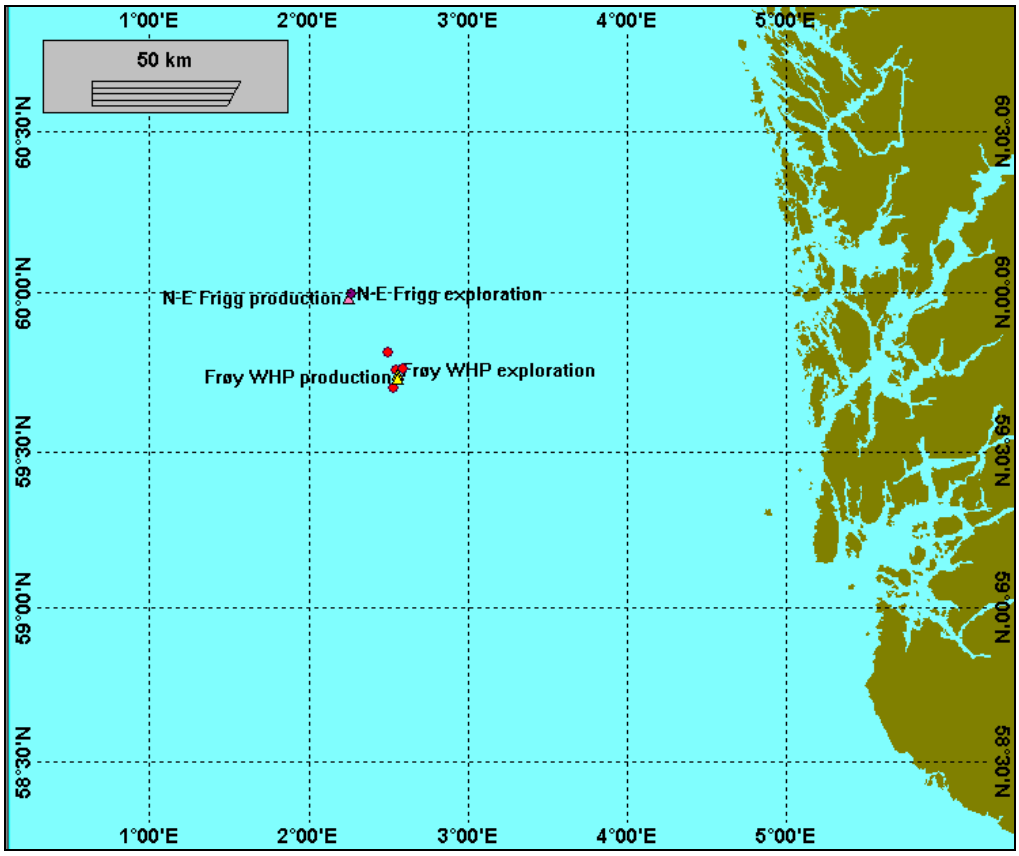


*Figure 3.7. The location of the two fields North-East Frigg and Frøy WHP.*

The numerical simulations were carried out in two steps:

- First, the discharges at the two sites were simulated, starting with the discharges from the top hole sections (36" and 26"). These discharges were assumed to be deposited directly on the sea floor. Then the discharges from the deeper well sections were simulated, assuming that these discharges took place from the platform (discharge depth will be close to the sea surface). Thus, a build-up of the cuttings piles on the locations was simulated as realistically as possible.

- Second, the piles were exposed to the winds and currents on the sites through a period of 4 - 5 years for re-suspension and redistribution of the cuttings material in the vicinity of the discharge sites.

After the period of 4 - 5 years with re-suspension of the cuttings piles, the results from the numerical simulations were compared with the field data collected in 1999.

For the simulation of the dormant period after the completion of the discharges, an ocean current data base for the North Sea for the years 1990 - 1994 were used (the OLF ocean current data base). The currents were generated by a hydrodynamic model operated by DNMI (*The Norwegian Meteorological Institute*) in Oslo. The ocean currents include residual currents, meteorological forcing as well as tidal motions. Time resolution is 2 hours and grid size is 20 km in the horizontal. The vertical resolution is variable with the depth, with a finer resolution close to the sea surface and with a coarser resolution close to the sea floor. Figure 3.8 shows one snapshot of the surface currents in the North Sea area generated from the DNMI ocean current model.

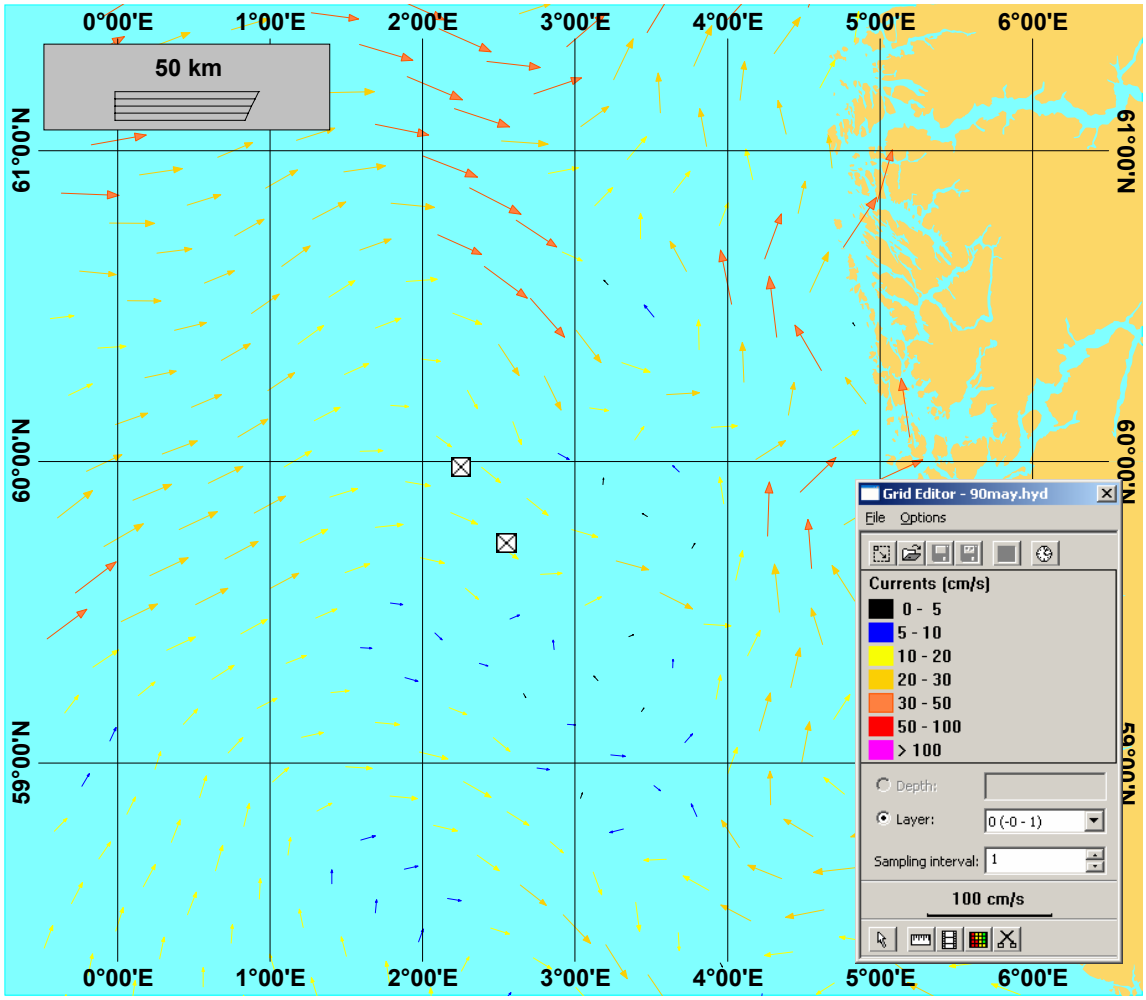


*Figure 3.8. Snapshot of ocean currents simulated with the DNMI model. Snapshot from May 1st, 1990, surface currents.*

For the generation of the waves, winds from the Gullfaks area (Tampen) were used. This data set contains wind direction and velocity for each 6th hour through the same 5 years as for the currents. This study is therefore based on an assumption that the winds and currents statistics for this period (1990 - 1994) is representative for the whole period where the cuttings piles have been dormant (until 1999).

For the calculation of the deposits of the cuttings on the sea floor, available data bases on the drilling locations through the years of activities were searched, both for exploration drilling and for production drilling.

For the North-East Frigg location, one exploration drilling location and 7 production drilling wells were detected in the area. The exploration drilling site was located far off the production drilling site and was therefore discarded. All 7 production wells had identical coordinates. Therefore these 7 wells were selected for the analysis.

For the Frøy WHP location, 5 exploration drilling locations and 12 production drilling wells were detected in the vicinity area. All the 5 exploration drilling sites were located off the production drilling site and were therefore discarded. Two of the 12 production wells had coordinates that deviated significantly from the other 10 production wells. The remaining 10 production wells were therefore selected to be included in the analysis. The locations selected were therefore all located rather close to each other (within a circle of radius 10 - 12 m) and could therefore be approximated with the same discharge location in the simulations.

Data for the discharges from these wells were collected with kind assistance from the oil company Total (formerly Elf) who operated these fields in the past. The discharges included for the North-East Frigg field are as follows. The cuttings material discharged from the upper well sections (deposited on the sea floor) amounted to 1343 tons (as an average for each well), while the cuttings material discharged from the deeper well sections (released from the drilling rig) amounted to 793 tons (as an average for each well). These discharges were repeated 7 times in the simulations in order to account for the total release of cuttings from the 7 wells at the North-East Frigg field. In total, 14 950 tons of cuttings were discharged in the model simulations.

The similar numbers for the Frøy WHP field are as follows. The cuttings material discharged from the upper well sections (deposited on the sea floor) amounted to 1396 tons (as an average for each well), while the cuttings material discharged from the deeper well sections (released from the drilling rig) amounted to 696 tons (as an average for each well). These discharges were repeated 10 times in the model simulations in order to account for the total release of cuttings from the 10 wells at the Frøy WHP field. In total, 20 920 tons of cuttings were discharged in the model simulations.

The cuttings particles were allowed to sink down in the sea floor according to their sizes and density. For the discharges deposited on the sea floor directly, the cuttings were deposited directly in the model grid cell corresponding to the discharge location. For the discharges from the platform, the size distribution of the cuttings particles needs to be known in order to calculate their sinking velocities properly. This size distribution is however not known, and must therefore be selected based on judgment. For the present simulations, the “default” grain size distribution was applied in the simulations. This distribution is shown in Table 3.2 (SINTEF, 2006).

*Table 3.2. Grain size distributions of cuttings particles (SINTEF, 2006)*

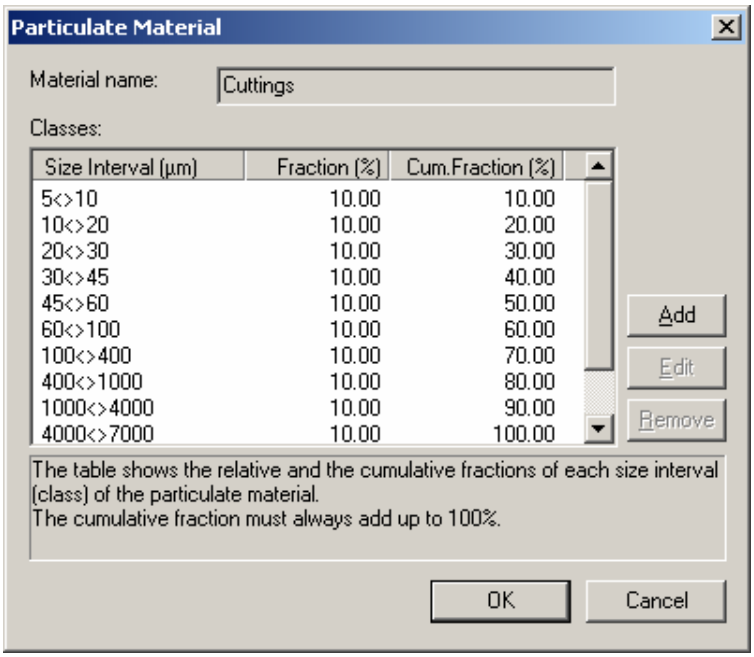


By consulting Stig Westerlund at Rogaland Research in Stavanger, who collected the samples in 1999, we were informed that the particle sizes in the mud/cuttings samples collected were apparently not large, and generally lower that order one mm. Therefore, the default particle size distribution was therefore selected which was based on the "default" particle size used in the ERMS project (SINTEF 2006), but redistributing all particle classes so that all diameters remained smaller than 1 mm. The resulting particle size distribution used in the simulations is shown in Table 3.3.

*Table 3.3. Alternative grain size distributions of cuttings particles and their sinking velocities, based on the assumptions that all particle sizes are lower than 1 mm for the Frøy WHP and the North-East Frigg simulations.*

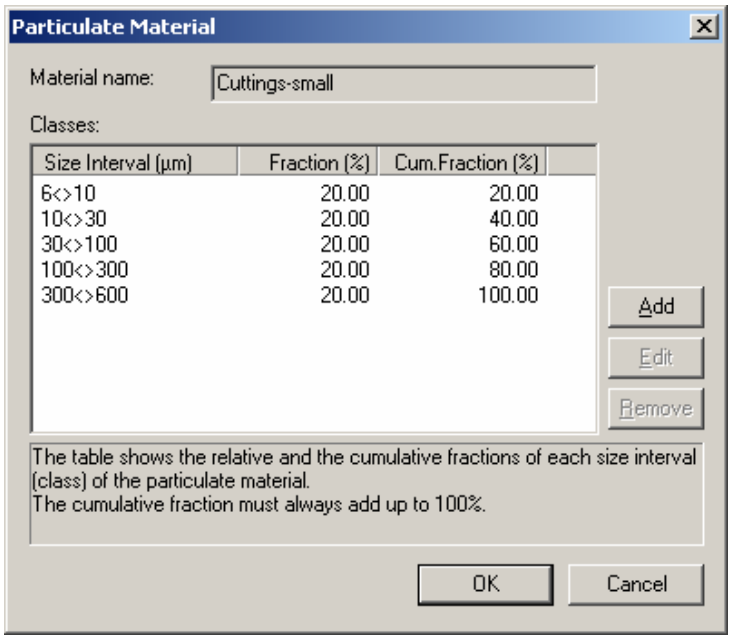


It may be mentioned that during the ERMS field survey, particles sizes of cuttings material were observed by ROV to be up to several mm in diameter during their descent down to the sea floor. However, these particles were not found again during the ERMS project sediment survey carried

out immediately after the completion of the drilling operations. One possible explanation to this finding may be that a large fraction of the rock drilled during the ERMS field survey (Sleipner Vest Alfa Nord field in the Sleipner region) consisted of clay and shalestone, which tend to resolve into smaller particles while they are deposited on the sea floor. It was also noted that the cuttings particles tended to resolve into smaller particles during the analysis of the particle sizes in the laboratory.

The particle size distribution is important for both the deposition and the re-suspension of the cuttings. Generally, larger particles re-suspend to a smaller extent, compared to smaller particles. Therefore, since these particle size distributions are not known, the assumptions made on the particle sizes add an extra uncertainty to the results from these simulations.

For the Frøy WHP case, the cuttings discharged from the rig were assumed to contain parts of a synthetic based drilling fluid (SBM) used during the drilling process. The amounts of discharge of the SBM were estimated to be more than 10 % weight of the cuttings discharged from the rig. According to Rogaland Research (2003), the amount of SBM discharged was 1254 $m^3$ (type Ultidrill, Linear alpha olefin) in total for the Frøy WHP production drilling. The SBM tends generally to have "sticky" properties, which will cause the discharge at the Frøy WHP field to form larger "clumps" through the discharge and deposition process. This process is denoted "agglomeration", and causes the cuttings particles discharged from the drilling rig to deposit relatively close to the release site due to the size of the clumps (several mm). This "agglomeration" process is built into the ERMS model, and was applied for the discharges from the platform at the Frøy WHP field.

### 3.5 Results for the North-East Frigg simulations (WBM discharge case)

After the simulations of the depositions on the drilling site were completed, the depositions on the sea floor were exposed to the winds and the currents through a time period of about 5 years. The combined action of the stresses exerted on the sea floor by the waves (given by the winds) and the currents (taken from the appropriate grid point in the hydrodynamic model simulations carried out by DNMI). The particles on the sea floor were re-suspended when the bottom stresses passed the criterion for the re-suspension (particle size dependent).

Only particles deposited on the sea floor originating from the cuttings discharged were re-suspended, leaving the original sediment undisturbed. This is not quite correct, because also the original sediment on the site may re-suspend during storms. The observations made in 1999 (shown in the Figures 3.5 and 3.6) indicate that re-suspension of the original sediment will take place and thus causes the added sediment to be located below the sediment surface. This process is however neglected in the simulations, leaving all the re-suspended sediment on top of the original sediment on the location.

The results from the model simulations on the North-East Frigg are illustrated by the Figures 3.9 – 3.11. Two sets of runs were carried out for the different particle size distributions of the cuttings as shown in the Tables 3.2 and 3.3 (coarse cuttings distribution and fine cuttings distribution, respectively).

Figure 3.9 shows the distribution of the deposited sediment at the end of the simulation period (in total 2019 days, or in excess of 5 years) for the case with coarse cuttings distributed and resuspended on the sea floor. For convenience, all discharges were performed through a time period of 7 months (one discharge for each month), which are considerably shorter than the total

drilling period on the site (over many years). In spite of that, the simulations show that the re-suspension and re-deposition have taken place during the discharge period as well. The figure shows the horizontal distribution of the cuttings after about 5 years of exposure, which is to be compared to the actual deposition on the site measured in 1999 as shown in Figure 3.5. The two figures are not directly comparable because the Figure 3.9 shows the deposition in kg/m$^2$ sediment surface, while Figure 3.5 shows the measured deposition in cm thickness of the cuttings layer. The figures become however comparable when it is noted that 1 cm of deposited matter corresponds approximately to 10 kg of cuttings deposited per m$^2$ sediment surface.

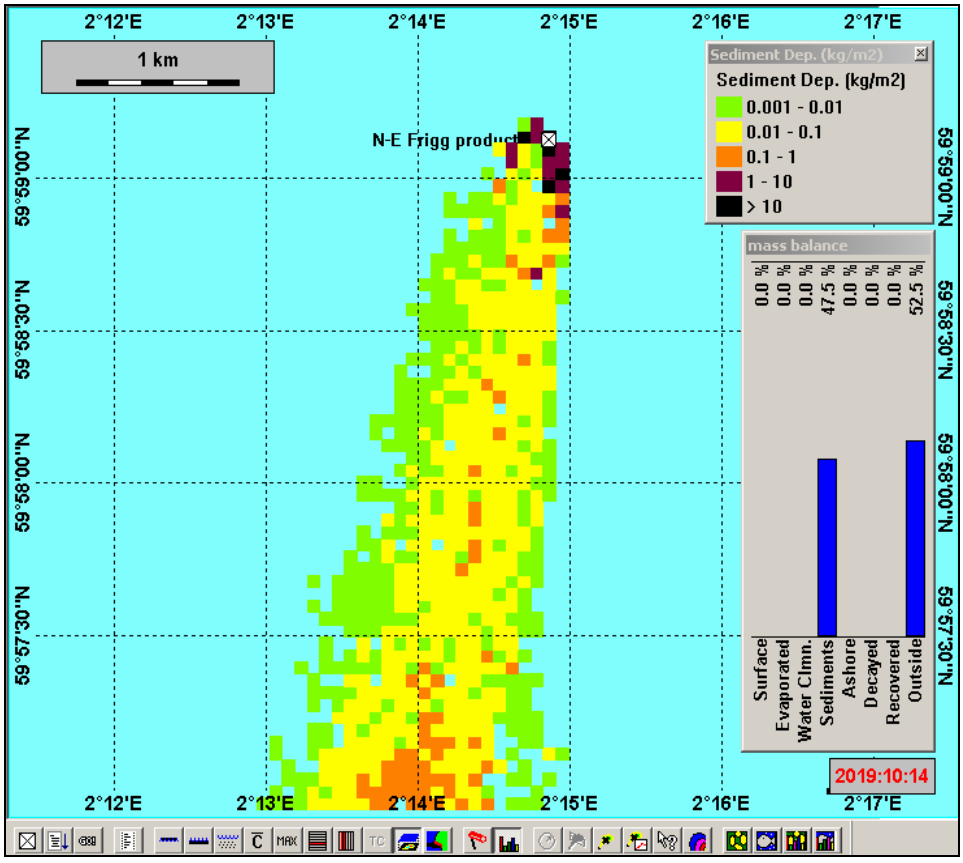


*Figure 3.9. North-East Frigg case. Deposited matter on the sea floor after 2019 days of simulation time. 10 kg of deposited matter corresponds approximately to 1 cm of thickness of cuttings layer (porosity 0.6 and density of cuttings 2500 kg/m$^3$).*

Note that the deposition remaining after 5 years is mostly limited to the grid cells closest to the discharge point. However, the amount of mass remaining in the model is substantially larger than the amount of mass measured in the sediment during the survey in 1999. In particular, the amount of mass in the grid cell at the discharge point contains a considerable amount of mass. Figure 3.10 shows the build-up of mass at the grid cell comprising the discharge point as the time development of the content of the grid cell. The build-up reaches about 1000 kg/m$^2$ of cuttings material. This amount corresponds to about 5600 tons of mass at that grid point (grid cell size is about 75m x 75m). This amount corresponds to about 38 % of the total discharge. This cell therefore contains a substantial amount of the mass remaining within the grid area (47.5 % in Figure 3.9).

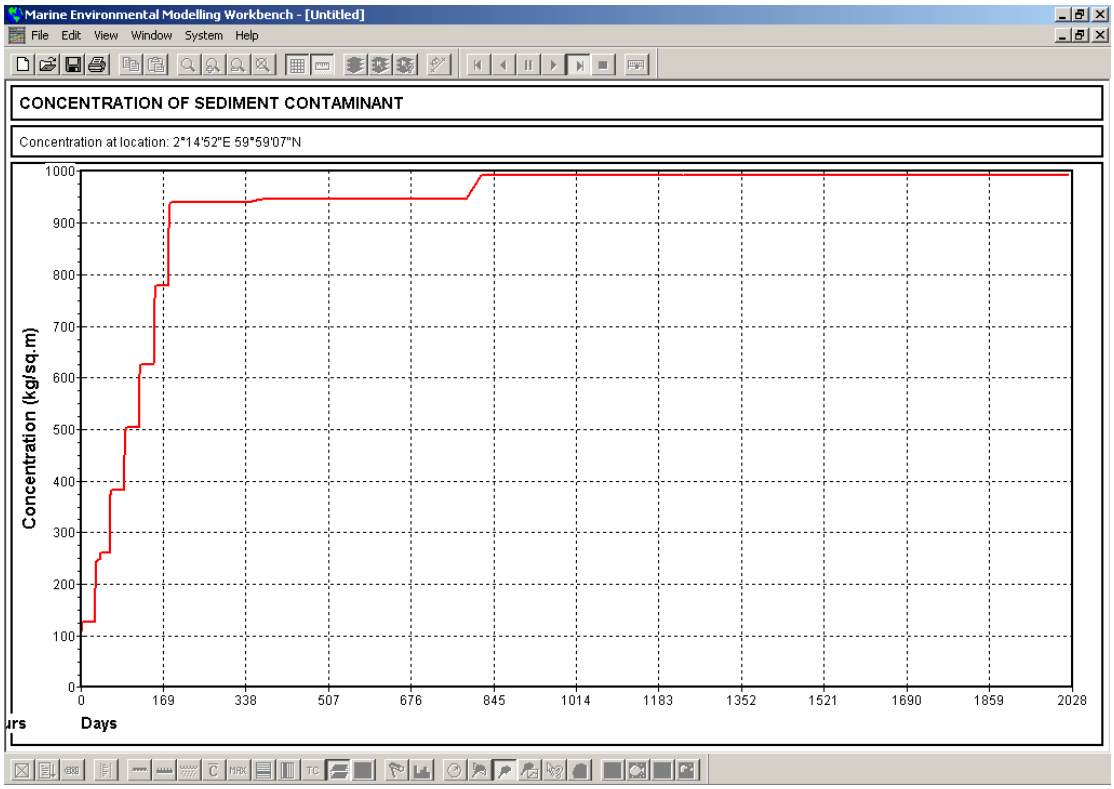


*Figure 3.10. North-East Frigg case. The build-up of cuttings at the grid cell containing the discharge point. Cuttings distribution is shown in Table 3.2 (large cuttings particles).*

Remaining mass observed during the 1999 survey was of order 100 kg/m$^2$ mass (or 10 cm height) within an area of order 75m x 75m (see Figure 3.5), which amounts to about 560 tons or about 10 % of the mass calculated within the same area with the model. The model therefore grossly overestimates the mass remaining at the site at North-East Frigg.

On the other hand, calculating the deposition and the re-suspension of the cuttings for the case that the grain size distribution contained much lower sized particles (as shown in Table 3.3) showed that nothing was left in the modeled area after the 5 years computer time. Figure 3.11 shows the deposited mass calculated for the grid cell that contained the discharge point. After some build-up, all of it is resuspended within a year or so.

The explanation of this is that the grain sizes have a large influence on the ability of the cuttings to resuspend. Small (unconsolidated) particles resuspend much easier than larger particles. When the larger particles are removed from the particle size distribution, the particles resuspend much more easily. Therefore, the results become very sensitive to the particle size distribution assumed. Since the particle size distribution is not known, this distribution has to be assumed. It is therefore possible to assume a particle distribution that will consist of a “mixure” of the particle size distributions shown in the Tables 3.2 and 3.3 that would result into a match with the observed content of the cuttings in the sediment during the survey in 1999.

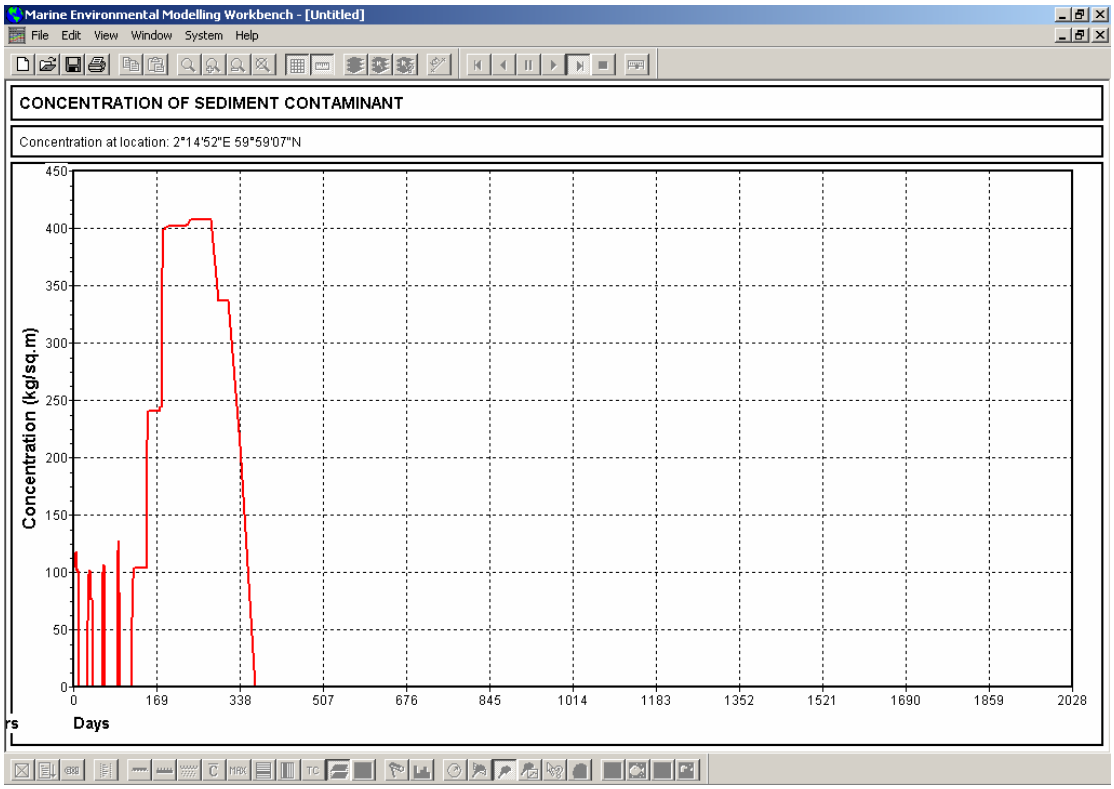


*Figure 3.11. North-East Frigg case. The build-up of cuttings at the grid cell containing the discharge point. Cuttings distribution is shown in Table 3.3 (Small cuttings particles).*

Also note that in Figure 3.9, there seems to be a continuous deposition of the cuttings in the southward direction. This is in agreement with the field results shown in Figure 3.5, which indicates no limit on the deposited remnants of the pile in the southward direction. This result may however be a coincidence, because the simulation results indicate that the main spreading direction of the cuttings material is very variable, dependent on the prevailing direction of the currents (although the southward direction of the transport of the cuttings material is dominating throughout the simulation period).

There is some dependency of the results on the choice of the time step in the model simulations. Based on experience, the re-suspension model should be run with a time step of order 10 - 20 minutes. This time step should be maintained throughout the whole simulation period (this happens automatically once the re-suspension button is chosen in the model, jointly with choosing the sediment button to be on as well). This time dependency is considered to be a weakness of the present version of the model. For the time being, the user is advised to select the time step in the simulations within the time interval 10 - 20 minutes, until more satisfactory algorithms are developed.

For the simulation results shown in this chapter, a time step of 10 minutes was combined with a grid size of 75m x 75m. There may also be some dependency of the grid size as well, because the height of the deposited layer on the drilling site is dependent on the size of the grid. The grid size chosen should therefore reflect the thickness of the layer expected from the masses deposited directly on the sea floor (while drilling the 36” and 26” sections of the well).

### 3.6 Results for the Frøy WHP simulations (SBM discharge case)

In the same way as for the North-East Frigg case, the depositions on the sea floor were exposed to the winds and the currents through a time period of about 5 years. The results from the model simulations on the Frøy WHP case are shown in the Figures 3.12 – 3.14. Two sets of runs were carried out for the different particle size distributions of the cuttings as shown in the Tables 3.2 and 3.3 (coarse cuttings distribution and fine cuttings distribution, respectively).

The deposition of the cuttings discharged from the drilling rig in the Frøy WHP case was assumed to consist of "agglomerated particles" with several mm i diameter. This agglomeration was due to the use of the synthetic based drilling fluid (SBM). The particle distribution for this part of the release was chosen according to Delvigne (1996) The cuttings material therefore deposited close to the discharge due to this agglomeration process. However, when the cuttings particles reached the sea floor, the cuttings particles regained their original size. This is not however quite realistic, because the "sticky properties" of the SBM are expected to maintain for some time after the discharge has reached down on the sea floor.

Figure 3.12 shows the distribution of the deposited sediment at the end of the simulation period (in total 2109 days, or in excess of 5 years) for the case with coarse cuttings distributed and resuspended on the sea floor. In this case, all discharges were performed through a time period of 10 months (one discharge for each month). In spite of that, the simulations show that the re-suspension and re-deposition have taken place during the discharge period as well in this case also. The figure shows the horizontal distribution of the cuttings after about 5 years of exposure, which is to be compared to the actual deposition on the site measured in 1999 as shown in Figure 3.6. The two figures are not directly comparable because the Figure 3.12 shows the deposition in $kg/m^2$ sediment surface, while Figure 3.6 shows the measured deposition in cm thickness of the cuttings layer. The figures become however comparable when it is noted that 1 cm of deposited matter corresponds approximately to 10 kg of cuttings deposited per $m^2$ sediment surface.

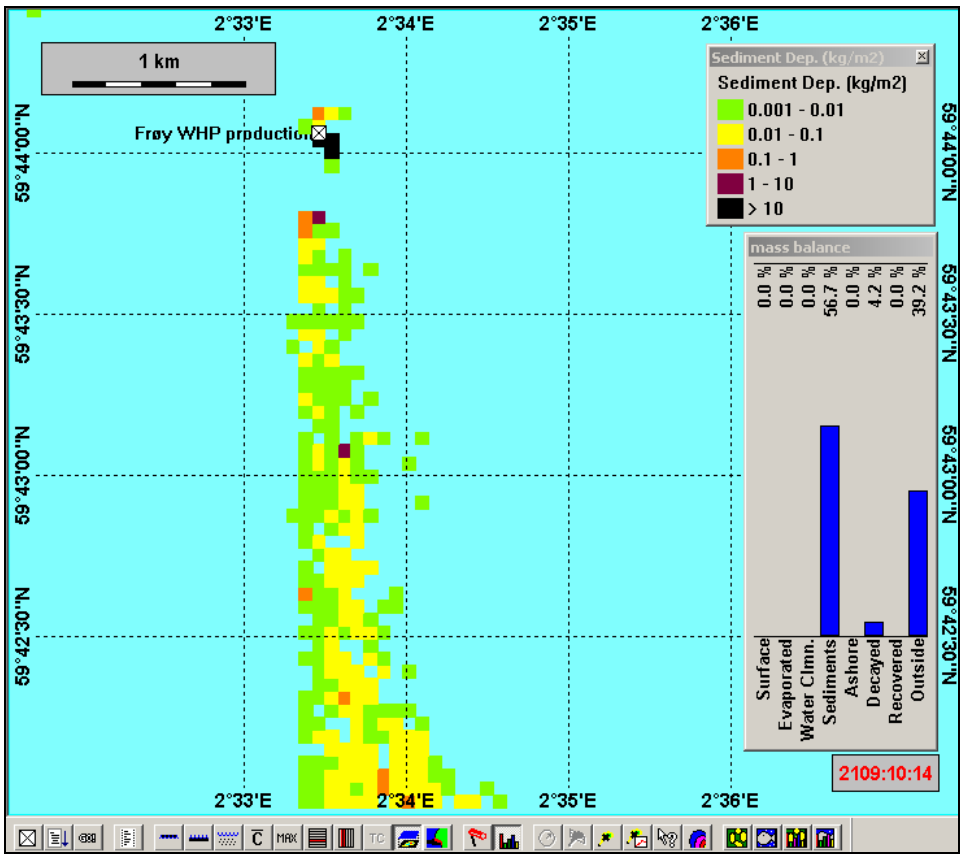


*Figure 3.12. Frøy WHP case. Deposited matter on the sea floor after 2109 days of simulation time. 10 kg of deposited matter corresponds approximately to 1 cm of thickness of cuttings layer (porosity 0.6 and density of cuttings 2500 kg/m$^3$).*

Again, the largest depositions remaining after 5 years are mostly limited to the grid cells closest to the discharge point. However, the amount of mass remaining in the model is substantially larger than the amount of mass measured in the sediment during the survey in 1999. In particular, the amount of mass in the grid cell at the discharge point contains a considerable amount of mass. Figure 3.13 shows the build-up of mass at the grid cell comprising the discharge point as the time development of the content of the grid cell. The build-up reaches about 2200 kg/m$^2$ of cuttings material. This amount corresponds to about 12 300 tons of mass at that grid point (grid cell size is about 75m x 75m). This amount corresponds to about 59 % of the total discharge. This cell therefore contains a substantial amount of the mass remaining within the grid area (56.7 % in Figure 3.12, but that number also includes the mass of the drilling mud).

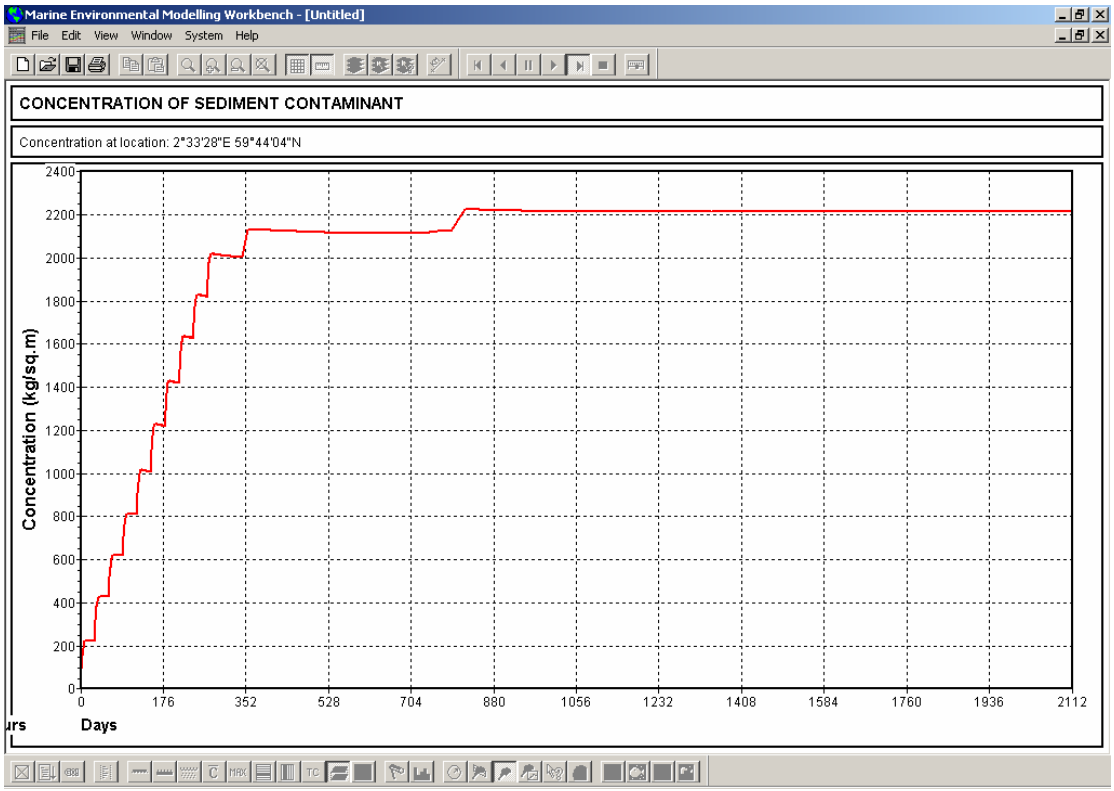


*Figure 3.13. Frøy WHP case. The build-up of cuttings at the grid cell containing the discharge point. Cuttings distribution is shown in Table 3.2 (large cuttings particles).*

Remaining mass observed during the 1999 survey was of order 100 kg/m$^2$ mass (or 10 cm height) within an area of order 150m x 150m (see Figure 3.6), which amounts to about 2 250 tons or about 20 % of the mass calculated within the same area with the model. The model therefore overestimates the mass remaining close to the drilling site for the Frøy WHP case also.

On the other hand, calculating the deposition and the re-suspension of the cuttings for the case that the grain size distribution contained much lower sized particles (as shown in Table 3.3) showed also in this case that nothing was left in the modelled area after the 5 years computer time. Figure 3.14 shows the deposited mass calculated for the grid cell that contained the discharge point. After some build-up, all of it is resuspended within a year or so.

A for the North-East Frigg case, it would therefore be possible to assume a particle distribution that will consist of a “mixure” of the particle size distributions shown in the Tables 3.2 and 3.3 that would result into a match with the observed content of the cuttings in the sediment during the survey in 1999 for the Frøy WHP case as well.

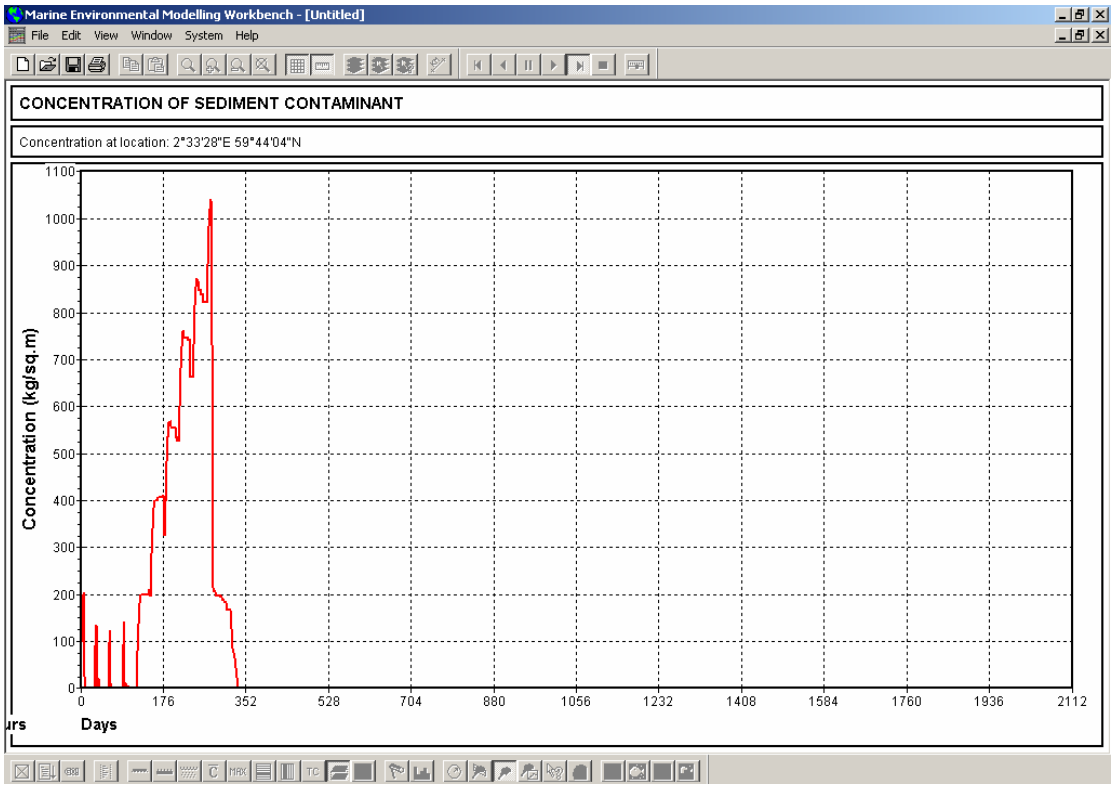


*Figure 3.14. Frøy WHP case. The build-up of cuttings at the grid cell containing the discharge point. Cuttings distribution is shown in Table 3.3 (Small cuttings particles).*

For the simulation results shown for the Frøy WHP case, a time step of 10 minutes was combined with a grid size of 75m x 75m. The grid size chosen should reflect the thickness of the layer expected from the masses deposited directly on the sea floor (while drilling the 36" and 26" sections of the well).

For the Frøy WHP case, the mass deposited in the grid cell that includes the discharge point will be substantially larger than for the North-East Frigg case. The reasons for this are three-fold. First, the number of wells drilled is larger (10 instead of 7 yielding 40% more discharge amount). Second, the discharge is expected to deposit closer to the well location due to the "agglomeration" process. And third, the mass of the drilling mud will deposit along with the cuttings (as a result of the agglomeration process). These three factors will cause a larger build-up of masses close to the drilling point, which is also reflected in the simulation results (compare the Figures 3.10 and 3.13) as well as in the field data from 1999 (compare the Figures 3.5 and 3.6).

### 3.7 Discussion

The resuspension model developed shows that the results are very sensitive to the assumption on the grain size distribution. These can vary a lot. The two distributions assumed in the present simulations are not “extreme”, but are both observed in the field. The distribution for the coarse cuttings was observed by Saga (Saga, 1994) during an exploration drilling in the Barents Sea, and the fine cuttings size distribution is rather similar to one of the cuttings distributions used by BMT in their UKOOA study of the cuttings piles in the North Sea (UKOOA 2002, Annex B).

The cuttings deposited on the sea floor are assumed to be “unconsolidated” in the model simulations, that is, the particles are assumed to behave independently of each other. No “bound” of any kind is assumed to be present between the particles. This will be true for freshly deposited (water based) sediment in particular, but some consolidation should be expected through a time period of 5 years. This should be in particular true for the Frøy WHP case, where SBM are expected to “attach” to the deposited cuttings particles. The carbon content of the (biodegradable) mud must also be expected to cause growth of “opportunistic fauna” on the pile, which, in turn, may increase the resistance of the pile to resuspend. A separate project financed by the Norwegian Research Council (NFR), the “PEIOFF” project, will address this issue, with the purpose of building into the ERMS model the faunal influence on the ability for the pile to resuspend (and also to arrive at bioturbation coefficients that will be flora and/or fauna dependent).

The ERMS model simulation result seems however to resolve an issue that came out of the UKOOA project that seems to be surprising: That the rate of loss of cuttings material from a pile seems to *increase* with water depth, rather than decreasing (UKOOA 2002, Figures 73 and 74). This is contrary to expectation, because it is generally believed that the wave action will have a larger influence on the loss rates (over the years) when the depths are smaller. This question may now be resolved by considering the influence of the particle size distributions. In the present study, the cuttings piles in the Frigg and Frøy areas were simulated with similar results at both locations. At these two locations, WBM and SBM were used. The water depths at the locations are 100 and 120 m, respectively. The remnants of the piles at these two locations were measured to be at maximum 10 - 15 cm high. This is contrasted to the results at the Ekofisk field, where the depths are shallower (around 70 m) but the cuttings piles have heights of order m. The explanation for this may now be attributed to the sizes of the “particles” that are deposited on the sea floor. If OBM are used, the discharges at the Ekofisk must be expected to form larger “clumps” or agglomerate. These clumps will be several mm in diameters (Delvigne, 1996). If these “clumps” are maintaining their identity once they are deposited on the sea floor, they may be very resistant to resuspension. In addition, the “clumps” may also attach to each other once deposited on the sea floor. Therefore, it would be possible to simulate OBM mud resuspension as well, by simulation of the “agglomeration” process (already included in the ERMS model) and also to include the identity of the “clumps” while they are deposited on the sea floor.

# 4 Re-colonization of the sediment layer

## 4.1 Introduction

Severe impact on the sediment layer may have fatal consequences for the biologic activity in the sediment layer. This may lead to a complete extermination of all biologic activities. Also, all effects caused by bioturbation (like mixing of sediment) may cease to occur. These effects are implemented in the model for the sediment layer developed as a part of the ERMS project as a reduction of the bioturbation coefficient (see model details in SINTEF, 2006).

When the toxic content in the sediment layer has biodegraded down to non-toxic levels, the sediment layer will start to recover after the discharge impact. Also, for the case where sediment composition and structure have been altered by the discharge, opportunists start to invade and replace the former benthic community.

The duration of impact on the sediment layer includes the time span from the first impact caused by a discharge until the sediment layer is recovered back to normal. The period of impact on the sediment layer therefore includes the period where the sediment layer is in the process of recovering from the impact.

The expected time period of recovery of a sediment layer should therefore be estimated. This chapter contains a review of information available in the literature. Based on this review, a discussion of the expected recovery time is given.

## 4.2 Review of selected references

NIVA, in their ERMS report (NIVA, 2006) considers the change of the diversity of the benthic community for locations where the THC (= Total Hydrocarbon Concentration) levels in the sediment layer have been reduced down to non-toxic levels. They note that after three years (that is, the time periods between two observations on the sites considered), the diversity index had returned back to normal levels. They therefore suggest that a three year time period might be used as a typical time span for a recovery time period of a sediment layer.

The Centre for Environment, Fishing and Aquaculture Science (CEFAS) reports in a four-year study on the seabed recovery after marine aggregate dredging. They write that (Marine Scientist, 2004) the “overall finding from this research is that recovery of some sites may take longer than the two to three years that previous research had suggested”. The article also points out that “the period taken for recovery appears to be dependent on both local environmental factors and the intensity of dredging”. This finding indicates that similar statements may be valid for depositions on the sea floor as well, which to some extent represents the “opposite action”, that is, to add mass on the sea floor rather than removing them.

Other sources also point out that the restitution time of the sediment layer may be longer than three years. Summary reports from the UKOOA project (see UKOOA 2003 and references therein) indicate that the restitution may take place in terms of successions. Preliminary stage communities may be established rapidly and within 1 – 2 years time. More stable communities may then be found on the site after 5 – 10 years. Dames & Moore and NIOZ (1999) summarized different experiences with re-colonization of cuttings piles, dependent on the controlling or

dominant factor for the impact (toxicity, organic enrichment, impacted by cuttings material). They provided a Table (reproduced in UKOOA 2003, Table 3.2) for the different time scales involved for the different stages experienced during a re-colonization process. Also they point out the importance of the invasion of opportunistic species as a first phase of a recovery process (first 1 – 4 years).

### 4.3 Discussion

A restitution time of *5 years* seems presently as a fair choice for a "default" restitution time for impacted sediment where the toxicity compounds in the sediment have biodegraded down to below toxic levels. For sediment that has been impacted by toxic compounds (heavy metals, chemicals) and/or compounds that may lead to organic enrichment (typically OBM and SBM), the restitution times may be considerably longer. For these cases, the sediment must biodegrade (and bioturbate) the toxic compounds and the organic enrichment down to below levels that represents any potential impact on the biota in the sediment layer. The 5 years restitution time should therefore be applied as an addendum to the calculated impact time duration caused by the toxic effects and/or the organic enrichment.

One case of special interest may be a case where the sediment has been impacted by cuttings particles only. This will often be a case where WBM has been used. The mud discharge for WBM will basically consist of PLONOR chemicals with some non-PLONOR chemicals included. However, the non-PLONOR chemicals are most commonly water soluble. These are therefore expected to dissolve in the water column. The cuttings particles are therefore expected to reach down on the sea floor with negligible amounts of chemicals attached to it. The cuttings particles have typical sizes that may deviate significantly from the diameters of the natural sediment on the location. In such a case, the sediment may be invaded by species that prefer the new diameters of the sediment introduced through the discharge of the cuttings (that causes a change of sediment composition and structure). The cuttings particles are generally inert, and their sizes may be so large that they will not be removed or redistributed by re-suspension processes. In such a case, the changed community due to the changed sediment grain size may end up as a permanent change. In such a case, the "impact" on the sediment may be considered as lasting for an infinite length of time because the community structure has been permanently changed. In case that it is the inert cuttings *only* that have any impact on the sediment (due to burial and change of grain size), a 5 year restitution time may be acceptable as well. This means that the new community is accepted as a "permanent change of state" in the sediment layer after a 5 years period of recovery time. This consideration should be valid only for the part of the sediment when the stressors are limited to burial and grain size change only.

This feature is presently implemented in the DREAM model. The practice should be reviewed when more information on this topic becomes available. A research project in Norway (Norwegian Research Council, NFR- PROOF – PEIOFF project) has recently been granted that will address this topic of restitution of a sediment layer after impact.

# 5 References

Berner, Robert A., 1980: “Early Diagenesis. A Theoretical Approach”. Princeton University Press.

Black, K.P., and C.E. Vincent, 2001: High-resolution field measurements and numerical modelling of intra-wave sediment suspension on plane beds under shoaling waves. Coastal Engineering, Vol. 42, pp. 173-197.

Boudreau, Bernard P., 1997: ”Diagenetic Models and Their Implementation. Modelling Transports and Reactions in Aquatic Sediments”. Springer-Verlag Berlin Heidelberg.

Dames and Moore and NIOZ, 1999: “UKOOA Drill Cuttings Initiative Research and Development Programme Activity 2.1. Faunal Colonization of Drill Cuttings Piles Based on Literature”. Report prepared for UKOOA Drill Cuttings JIP dated 1999.

Delvigne, G.A.L., 1996: “Laboratory investigations on the fate and physiochemical properties of drill cuttings after discharge to the sea”. Pages 16 – 24 in “The Physical and Biological Effects of Processed Oily Drill Cuttings” (Summary Report). E & P Forum, London, 1996.

Fredsøe, J. and R. Deigaard, 1992: Mechanics of Coastal Sediment Transport. Advanced series on Ocean Engineering – Volume 3, World Scientific, Singapore, New Jersey, London, Hong Kong.

P.E. Holloway, P.E, and B. Barnes, 1998: A numerical investigation into the bottom boundary layer flow and vertical structure of internal waves on a continental slope. Continental Shelf Research, Vol. 18, pp 31-65.

Ichiye, T., 1967: Upper ocean boundary-layer flow determined by dye diffusion. Boundary Layers and Turbulence – The Physics of Fluids Supplement, pp. 270-277.

Kuhrts, C., W. Fennel, and T. Seifert, 2004: Model studies of transport of sedimentary material in the western Baltic. Journal of Marine Systems, Vol. 52, pp. 167-190.

Marine Scientist: “How quickly does the seabed recover after dredging”. Page 5, Marine Scientist No.8 3Q, 2004.

NIVA, 1997: “Biodegradation of Esters and Olefins in Drilling Mud Deposited on Arctic Soft-bottom Communities in a Low-temperature Mesocosm”. Report SNO 3760-97 dated 15 December 1997. NIVA project report for Saga Petroleum.

NIVA, 2006: “Remediation of sediments contaminated with drill cuttings. A review of field monitoring and experimental data for validation of the ERMS sediment module”. ERMS Report No. 22. NIVA Serial Report SNO 5188-2006. NIVA report O-25056 dated 15 March 2006.

OLF, 2001: “Information on Cuttings Piles on the Norwegian Continental Shelf”. OLF report 773/65 48 53 dated 24 January 2001.

Rogaland Research, Norway, 2003: “Environmental investigation of cuttings deposited in the Frigg area”. RF report RF-2000/219. Report prepared for Total dated 24 November 2003.

Saga Petroleum, 1994: “Miljøprogram I forbindelse med brønn 7219/8-1s i Barentshavet”. Report from Saga Petroleum R-TIY-0003 dated March 1994. Written in Norwegian.

Shimmield, G. B. et. al., 2000: “Contaminant Leaching from Drill Cuttings Piles of the Northern and Central North Sea: Field results from the Beryl cuttings pile”. Scottish Association for Marine Life, Centre for Coastal and marine Sciences.

SINTEF, 1999: “Simulated Seabed Study – Establishment of Test Systems and Guideline”. SINTEF report STF66 F99131 dated 6 December 1999. Project report for OLF and three oil companies.

SINTEF, 2006: “Documentation report for the revised DREAM model. Final version, August 2006”. ERMS Report No. 18 dated 31 August 2006.

UKOOA, 2003: “Drill Cuttings Initiative. Food Chain Effects Literature Review”. Report prepared for UKOOA Drill Cuttings JIP dated January 2003.

UKOOA, 2002: “Drill Cuttings Initiative Phase II. Task 4. Adaption and Evaluation of Mathematical Model”. UKOOA Report No. 14900/00 dated February 2002.

Zyserman, J.A, and J. Fredsøe, 1994: Data analysis of bed concentration of suspended sediments. Journal of Hydraulic Engineering, Vol. 120, pp. 1021-1042